Petroleum Science 20 (2023) 2354–2371

Contents lists available at ScienceDirect

Petroleum Science

journal homepage: www.keaipublishing.com/en/journals/petroleum-science

Original Paper

Production characteristics and displacement mechanisms of infilling polymer-surfactant-preformed particle gel flooding in post-polymer flooding reservoirs: A review of practice in Ng3 block of Gudao Oilfield

Zhi-Bin An [a, c], Kang Zhou [b, **], De-Jun Wu [a, c], Jian Hou [a, c, *]

[a] Key Laboratory of Unconventional Oil & Gas Development (China University of Petroleum (East China)), Ministry of Education, Qingdao, 266580, Shandong, PR China
[b] College of Energy and Mining Engineering, Shandong University of Science and Technology, Qingdao, 266590, Shandong, PR China
[c] School of Petroleum Engineering, China University of Petroleum (East China), Qingdao, 266580, Shandong, PR China

ARTICLE INFO

Article history:
Received 24 June 2022
Received in revised form
22 December 2022
Accepted 26 December 2022
Available online 29 December 2022

Edited by Yan-Hua Sun

Keywords:
Infilling polymer-surfactant-PPG flooding
Production characteristics
Displacement mechanisms
Dimensionless seepage resistance
Water absorption profile

ABSTRACT

The pilot test of infilling polymer-surfactant-preformed particle gel (PPG) flooding has been successfully implemented after polymer flooding in Ng3 block of Gudao Oilfield in China. However, the production characteristics and displacement mechanisms are still unclear, which restricts its further popularization and application. Aiming at this problem, this paper firstly analyzes the production performance of the pilot test and proposed four response types according to the change of water cut curves, including W-type, U-type, V-type response, and no response. Furthermore, the underlying reasons of these four types are analyzed from the aspects of seepage resistance and sweep efficiency. The overall sweep efficiency of gradual-rising W-type, gradual-decreasing W-type, and early V-type response increases from 0.81 to 0.93, 0.55 to 0.89, and 0.94 to 1, respectively. And the sum of seepage resistance along the connection line between production well and injection well for U-type and delayed V-type response increases from 0.0994 to 0.2425, and 0.0677 to 0.1654, respectively. Then, the remaining oil distribution after polymer flooding is summarized into four types on the basis of production and geological characteristics, namely disconnected remaining oil, streamline unswept remaining oil, rhythm remaining oil, and interlayer-controlled remaining oil. Furthermore, the main displacement mechanisms for each type are clarified based on the dimensionless seepage resistance and water absorption profile. Generally, improving connectivity by well pattern infilling is the most important for producing disconnected remaining oil. The synergistic effect of well pattern infilling and polymer-surfactant-PPG flooding increases the dimensionless seepage resistance of water channeling regions and forces the subsequent injected water to turn to regions with streamline unswept remaining oil. The improvement of the water absorption profile by polymer-surfactant-PPG flooding and separated layer water injection contributes to displacing rhythm remaining oil and interlayer-controlled remaining oil. Finally, the paper analyzes the relationships between the remaining oil distribution after polymer flooding and production characteristics of infilling polymer-surfactant-PPG flooding. The study helps to deepen the understanding of infilling polymer-surfactant-PPG flooding and has reference significance for more commercial implementations in the future.

1. Introduction

As a mature chemical flooding technology, polymer flooding is still one of the effective methods to enhance oil recovery after water flooding. It can improve the sweep efficiency of the displacement fluid by injecting high viscosity solution, thus achieving the purpose of improving oil recovery of high water cut

* Corresponding author. Key Laboratory of Unconventional Oil & Gas Development (China University of Petroleum (East China)), Ministry of Education, Qingdao, 266580, Shandong, PR China.
** Corresponding author.
E-mail addresses: zhoukang_upc@163.com (K. Zhou), houjian@upc.edu.cn (J. Hou).

https://doi.org/10.1016/j.petsci.2022.12.010

reservoirs (Hou, 2007; Ma et al., 2017; Lu et al., 2021; Zhou et al., 2013). However, it is found that the effect of polymer flooding is weakened after the subsequent water flooding through a large number of field tests, resulting in a rapid increase in water cut and a significant decrease in oil production. What is worse is that the reservoir heterogeneity becomes more serious and the remaining oil is more dispersed after polymer flooding. The current chemical flooding technology is difficult to meet the requirements of further significant enhanced oil recovery (Imqam et al., 2017; Lu et al., 2014; Sheng et al., 2015; Wang, 2013; Zhong et al., 2022).

To further develop the remaining oil after polymer flooding, researchers propose a new displacement system by mixing polymer, surfactant, and PPG (Cao, 2013). PPG is a kind of profile control agent with expansion and deformation properties and shows the characteristics of discontinuous phase seepage in the formation. It is formed by mixing monomers, crosslinking agents, and initiators (Bai et al., 2007). It can increase the resistance coefficient, strengthen the flow diversion, and expand the swept area (Bai et al., 2007, 2015; Elsharafi and Bai, 2016; Hou et al., 2019). When it flows to the pore throat, it can cause blockage and force subsequent fluid flow to other layers, reflecting an increase in the displacement pressure difference. The displacement pressure difference gradually increases until it exceeds the extrusion pressure of PPG, then it can pass through the pore throat. Therefore, the composite system of PPG, polymer, and surfactant can adjust the heterogeneity of the reservoir, so that the displacement fluid can enter the unswept area and improve the sweep efficiency and displacement efficiency (Du et al., 2019; Song et al., 2018; Sun et al., 2018; Wu et al., 2020).

Aiming at the characteristics of high temperature, high water salinity, and strong heterogeneity of the reservoir in Shengli Oilfield, researchers developed a polymer-surfactant-PPG system that meets the conditions and a pilot test of that system was carried out in Ng3 block of Gudao Oilfield in 2010. It is worth noting that the well pattern was infilled in the block before polymer-surfactant-PPG flooding. This block is selected as the pilot test for polymer-surfactant-PPG flooding mainly include the following reasons. Firstly, the polymer flooding in the block has completed, and the production characteristics are in accord with the general laws of polymer flooding in Shengli Oilfield. Secondly, the reservoir fluid properties, temperature, and other characteristics can represent the reservoir after polymer flooding in Shengli Oilfield. Finally, the well pattern and injection-production relationship are relatively complete. By 2013, the comprehensive water cut in the pilot test area decreased by 18.5% compared with the maximum value, and the oil recovery increased by 3.5% (Sun, 2014). With the successful implementation of the pilot test, it is proved that polymer-surfactant-PPG flooding is one of the effective methods to further enhance oil recovery after polymer flooding. At present, the polymer-surfactant-PPG flooding technology has been industrially applied in some oilfields, and the effect of water reduction and oil increment is remarkable (Cao et al., 2017; Qiu et al., 2017; Seidy Esfahlan et al., 2021; Sun et al., 2020).

Since the polymer-surfactant-PPG flooding has achieved such good performance in field tests, many scholars have conducted a large number of further studies on the enhanced oil recovery mechanism of PPG, including the properties of PPG (Goudarzi et al., 2015; Moghadam et al., 2012; Saghafi et al., 2016), injection capability (Imqam et al., 2016; Zhang and Bai, 2011), migration capability (Farasat et al., 2017; Imqam et al., 2015), and others. At the same time, the classical seepage theory and lattice Boltzmann method are also proposed to study the profile control of PPG (Zhou et al., 2017, 2019). However, current researches mainly focus on micro and macro laboratory experiments and numerical simulations without combining a large amount of test data and production data obtained from oilfields, resulting in limited conclusions.

By June 2020, the pilot test of infilling polymer-surfactant-PPG flooding has been carried out for nearly ten years, and a large amount of test data and production data have been obtained. Therefore, this paper studies the production characteristics and displacement mechanisms of infilling polymer-surfactant-PPG flooding combining the pilot test data and numerical simulations.

2. Introduction of the pilot test

The pilot test area of polymer-surfactant-PPG flooding is located in the southeast of Ng3 block of Gudao Oilfield, which is a loose sandstone and hydrophilic reservoir. The reservoir is a positive rhythm deposition of fluvial facies with serious heterogeneity, and the reservoir properties are shown in Table 1. The pilot test area was put into production in September 1971 and transferred to water flooding in September 1974. After well pattern adjustment in 1983 and 1987, a 270 m × 300 m staggered row well pattern was formed. The polymer flooding pilot test was carried out in October 1992 and completed in December 2005, followed by the subsequent water flooding. Before the implementation of polymer-surfactant-PPG flooding in the pilot test area, the comprehensive field water cut was 98.3%, and the oil recovery was 52.3% (Sun, 2014).

The water channeling regions were formed after polymer flooding and subsequent water flooding in the pilot test area, which is difficult for further increasing the swept volume. Therefore, it was necessary to infill the well pattern before the implementation of polymer-surfactant-PPG flooding. According to the principle of well pattern adjustment, the original staggered row well pattern was infilled and adjusted to facing row well pattern, as shown in Fig. 1. Therefore, a 150 m × 135 m facing row well pattern was formed. As can be seen from Fig. 1, 8 production wells and 9 injection wells were infilled, and the streamline direction of the original well pattern was changed after well pattern infilling. The infilled well was put into production in July 2010, and the pre-slug of polymer and PPG was injected in October 2010. The injection volume was 0.08 PV, and the average concentration of polymer and PPG was 1660 mg/L. The main slug was injected in November 2011 with an injection volume of 0.3 PV. The average concentration of polymer and PPG was 1339 mg/L, and the surfactant concentration was 0.4%. After the injection of polymer, surfactant, and PPG, the average injection pressure increased from 7.6 to 10.2 MPa, while the polymer flooding in the same reservoir only increased by 0.8 MPa (Sun, 2014). By the end of polymer-surfactant-PPG flooding in January 2016, the pilot test entered the subsequent water flooding development stage. By June 2020, the cumulative enhanced oil recovery by infilling polymer-surfactant-PPG flooding in the pilot test area was 8.5%, and the oil recovery was as high as 63.6%.

There are great differences in the performance of each production well after the implementation of infilling polymer-surfactant-PPG flooding in the pilot test area. Therefore, four types of production characteristics are summarized and shown in Fig. 2 according to the water cut curve of ten production wells, including W-type response, U-type response, V-type response, and no response. The W-type response includes gradual-rising W-type response and gradual-decreasing W-type response. Gradual-rising W-type response includes producers 11XN411 and 11X3013, and gradual-decreasing W-type response includes producer 10X3010. The difference between these two types is that the W-type change occurs in the rising or decreasing stage of the water cut. The U-type response includes producer 12X3012, which is characterized by a deep water cut funnel and rapid decreasing and rising of water cut. The V-type response includes early V-type response and delayed V-type response. Early V-type response includes producers 9X3009 and 12X3013. The characteristic of this type is that the water cut has an early decreasing time. Delayed V-type response includes

Table 1
Reservoir properties in the pilot test area.

Parameter	Value	Parameter	Value
Depth, m	1173–1230	Oil covering area, km^2	0.275
Geological reserves, 10^4 t	123	Formation pressure, MPa	12
Crude oil viscosity, mPa s	46.3	Temperature, °C	69.5
Average porosity, %	33	Permeability, 10^{-3} μm^2	1500–2500
Formation water salinity, mg/L	5923	Crude oil volume factor	1.105

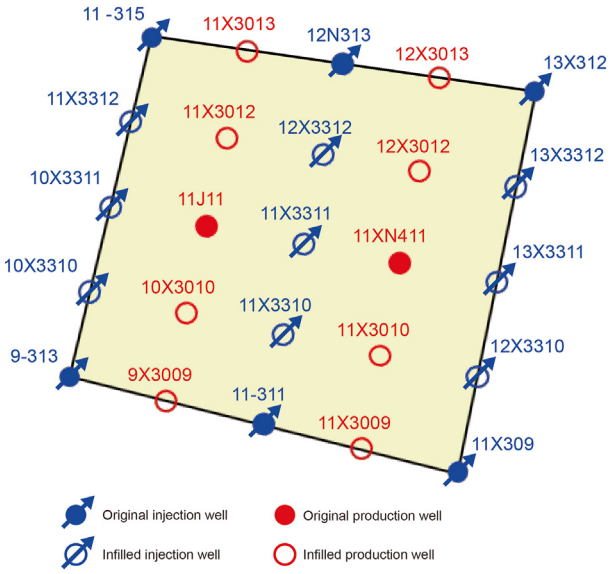

Fig. 1. Schematic diagram of the well pattern in the pilot test area.

producers 11J11, 11X3012, and 11X3009. Compared with the early V-type response, this type is characterized by a later decreasing time of water cut. No response includes producer 11X3010, which is characterized by no significant decrease in water cut. Noticeably, the water cut curves of each production well are unified to a fixed time since the model includes original wells and infilled wells with different opening times. Therefore, there are no data in the early stage for infilled wells. In this paper, the starting time of the curve is set to February 2009, and the ending time is set to June 2020 according to the production data. At the same time, some production wells are shut-in intermittently during the development process due to sand stuck, break off, and other working conditions, resulting in the discontinuity of water cut curves. Table 2 summarizes the opening and shut-in time of each production well, among which producers 11J11, 11X3010, and 12X3013 have been shut in due to high water cut.

Although four types of response are summarized according to the characteristics of the water cut curve of infilling polymer-surfactant-PPG flooding, it is unclear the reasons for these four types of response, as well as the differences and relations among them. Therefore, a numerical simulation model is established based on the production data and test data of the pilot test area. The production characteristics and displacement mechanisms of infilling polymer-surfactant-PPG flooding are analyzed based on the numerical simulation model.

3. Production characteristics and underlying reasons

Fig. 3 shows the numerical simulation model of infilling polymer-surfactant-PPG flooding in the pilot test area. Based on the production data and test data, the start time of the simulation is set to February 2009, and the end time is set to June 2020. The model adopts corner grids with a total of $97 \times 95 \times 52 = 479180$ grids, and the number of effective grids is 130391. Additionally, layers 18, 26, 34, and 44 in the Z direction are set as interlayers. The physical parameters of the reservoir changed greatly after water flooding and polymer flooding. The average porosity increases from the initial of 33%–36.7%, and the average permeability increases to 2589×10^{-3} μm^2. The average formation pressure drops to 10.67 MPa, and the average oil saturation is 32.36%. Other properties are shown in Table 1. It is worth noting that injection wells are shown in blue and production wells in red, and infilled wells are marked with "*" after the well name. In addition, the model area is expanded by 1–3 rows of grids in the X and Y directions since the model is partially intercepted from the whole block, which aims to reflect the fluid and energy exchange between the simulation model area and the external area.

Based on the injection dynamics of the polymer-surfactant-PPG system in the pilot test area, the slug settings during the development process are shown in Table 3.

In order to clarify the underlying reasons of production characteristics, the changes in seepage resistance and sweep efficiency before and after infilling polymer-surfactant-PPG flooding are calculated. On this basis, the characteristics of four types of response are analyzed combined with the remaining oil distribution at the characteristic points of the water cut curve.

(1) Seepage resistance

The seepage resistance reflects the flow resistance of the underground fluid during the seepage process in the porous medium. Based on the change of seepage resistance before and after infilling polymer-surfactant-PPG flooding, the characteristics of different types of response can be represented combined with the streamline. According to Darcy's law, the seepage resistance calculation equation can be calculated as follows:

$$R^{i,j} = \frac{1}{K^{i,j}\left(\frac{K_{ro}(S_w^{i,j})}{\mu_o^{ij}} + \frac{K_{rw}(S_w^{i,j})}{\mu_w^{ij}}\right)} \tag{1}$$

where $R^{i,j}$ and $K^{i,j}$ are the seepage resistance and absolute permeability of the grid (i, j); $K_{ro}(S_w^{i,j})$ and $K_{rw}(S_w^{i,j})$ are the relative permeability of the oil phase and water phase, both are functions of water saturation; μ_o^{ij} and μ_w^{ij} are the viscosity of the oil phase and water phase.

(2) Sweep efficiency and displacement efficiency

The sweep efficiency refers to the ratio of the swept volume of the injected fluid to the total volume of the reservoir, and the displacement efficiency refers to the ratio of the volume of crude oil displaced by the injected fluid to the original volume of the swept area. The sweep efficiency and displacement efficiency of infilling polymer-surfactant-PPG flooding can be calculated by counting the

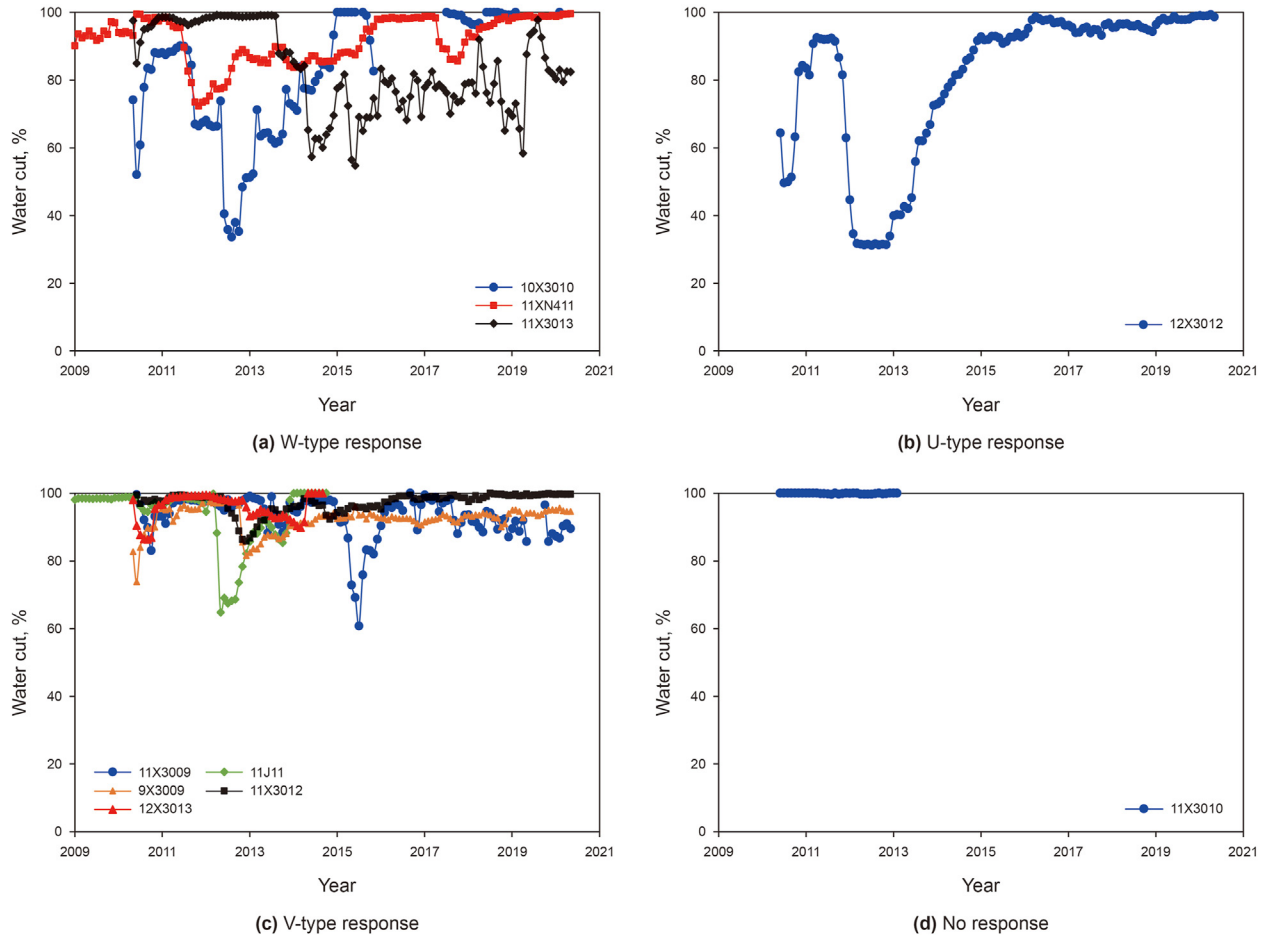

Fig. 2. Four types of production characteristics.

Table 2
The opening and shut-in time of production wells.

Well name	Opening time	Shut-in time	Well name	Opening time	Shut-in time
10X3010	2010.06	–	12X3013	2010.06	2014.10
11X3012	2010.07	–	12X3012	2010.07	–
11J11	2009.02	2014.11	11X3013	2010.06	–
11X3009	2010.07	–	11XN411	2009.02	–
11X3010	2010.07	2013.03	9X3009	2010.06	–

saturation field and pressure field before and after that.

In order to calculate the sweep efficiency and displacement efficiency resulting from infilling polymer-surfactant-PPG flooding, it is necessary to exclude the elastic production due to the drop of formation pressure assuming that the formation is elastic. When the formation pressure drops to P, the change of oil saturation per unit rock pore volume due to elasticity is (Wang, 2013):

$$\Delta V = \Big(C_f + \phi(S_{oi}C_o + S_{wc}C_w)\Big)S_{oi}(P_{init} - P) \tag{2}$$

where ΔV is the oil saturation change; C_f, C_w, and C_o are the compressibility coefficients of rock, water, and oil, respectively; S_{wc} and S_{oi} are the bound water saturation and initial oil saturation; P_{init} is the original formation pressure; ϕ is porosity.

Let $C_t = C_f + \phi(S_{oi}C_o + S_{wc}C_w)$, then the oil saturation reduction without elasticity in grid (i,j) can be calculated as follows (Wang, 2013):

$$\Delta S_o^{i,j} = S_{oi}^{i,j} - S_o^{i,j} - C_t S_{oi}^{i,j}\left(P_{init}^{i,j} - P^{i,j}\right) \tag{3}$$

Since the displacement efficiency, ED, represents the degree to which the injected fluid displaces the crude oil in the pores, the calculation equation can be expressed as:

$$ED = \frac{\Delta S_o^{i,j}}{S_{oi}^{i,j}} \tag{4}$$

Fig. 4 shows the frequency distribution and cumulative frequency distribution of displacement efficiency before and after infilling polymer-surfactant-PPG flooding. It can be seen from the figure that most of the displacement efficiency before infilling polymer-surfactant-PPG flooding is in the range of 0.3–0.7, which is generally low. After that, the displacement efficiency is concentrated in the range of 0.5–0.8, showing a significant improvement.

According to Fig. 4, it can be seen that the cumulative frequency

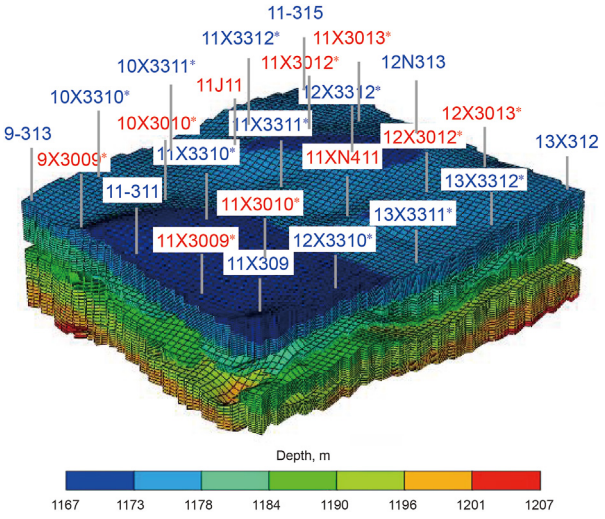

Fig. 3. The reservoir numerical simulation model.

Table 3
The slug settings during the development process.

Time	Slug
2009.02–2010.10	Water
2010.11–2011.07	1500 mg/L polymer + 1500 mg/L PPG
2011.08–2011.10	2000 mg/L polymer + 2000 mg/L PPG
2011.11–2011.12	900 mg/L polymer + 900 mg/L PPG + 0.4% surfactant
2012.01–2015.12	1200 mg/L polymer + 1200 mg/L PPG + 0.4% surfactant
2016.01–2020.06	Water

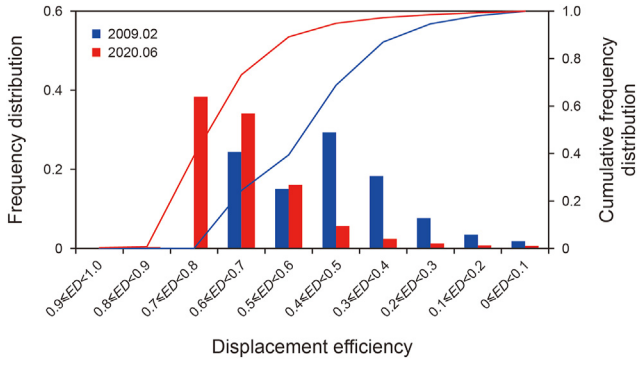

Fig. 4. Frequency distribution and cumulative frequency distribution of displacement efficiency.

distribution curve before and after infilling polymer-surfactant-PPG flooding almost keeps unchanged when the displacement efficiency is greater than 0.25. Therefore, the grid is considered to be effectively swept if its displacement efficiency is greater than 0.25 in the calculation of sweep efficiency. Since the physical properties and production performance of different well groups in the model are quite different, the model is divided into ten areas with each production well at the center. In the calculation of sweep efficiency, the pore volume of each grid in each area is counted, and the ratio of the sum of that with displacement efficiency greater than 0.25 to the sum of that of all grids in the area is calculated. The calculation equation is shown as follows:

$$EV = \frac{\sum PORV(ED > 0.25)}{\sum PORV} \tag{5}$$

where EV is sweep efficiency; $PORV$ is the pore volume of each grid; ED is displacement efficiency.

It is worth noting that the oil saturation in some grids may become larger due to the migration of the remaining oil, which causes the wrong decrease of grid displacement efficiency directly calculated using Eq. (5) and brings errors to the statistical analysis. In order to solve this problem, the swept condition of the grid before infilling polymer-surfactant-PPG flooding is used as the benchmark in the calculation process. That is to say, it can be considered that the grid has been swept if the displacement efficiency is greater than 0.25 in February 2009, even if it decreases in the subsequent development resulting from the migration of the remaining oil.

3.1. W-type response

3.1.1. Gradual-rising W-type response

There are two reasons for gradual-rising W-type response according to the remaining oil distribution at different times in the numerical simulation. Firstly, the remaining oil saturation around the production well is low after polymer flooding, and it takes a long time to displace the remaining oil from other areas to the production well. Secondly, the amount and the reaching time of the remaining oil migrating from different areas to the production well are different. Taking producer 11XN411 as an example, Figs. 5–7 show the water cut curve, the vertical distribution of remaining oil at 4 time points, and the sweep efficiency of perforating layers at 3 time points, respectively. It can be seen from Fig. 5 that the water cut is relatively high in the early stage, and it decreases to 72.3% after infilling polymer-surfactant-PPG flooding. Then it rises to 87.6% in November 2012 and remains relatively flat until it rises again in July 2015. From Fig. 6(a), it can be seen that the remaining oil saturation around producer 11XN411 is low after long-term water flooding and polymer flooding since it is an original production well, while the area far from the well is high. Then, the remaining oil far from producer is displaced to the well under the synergistic effect of profile control by polymer-surfactant-PPG system and streamline adjustment by well pattern infilling. But the oil amount displaced from each layer is different. As can be seen from Fig. 6(b–d) and Fig. 7, the remaining oil in the lower and upper layers is almost simultaneously displaced to the producer, as a result the water cut decreases rapidly to the lowest level. When the remaining oil displaced from the lower layers has been fully

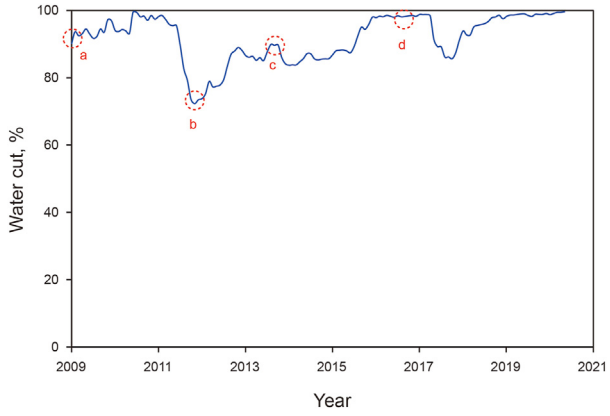

Fig. 5. Water cut curve of producer 11XN411.

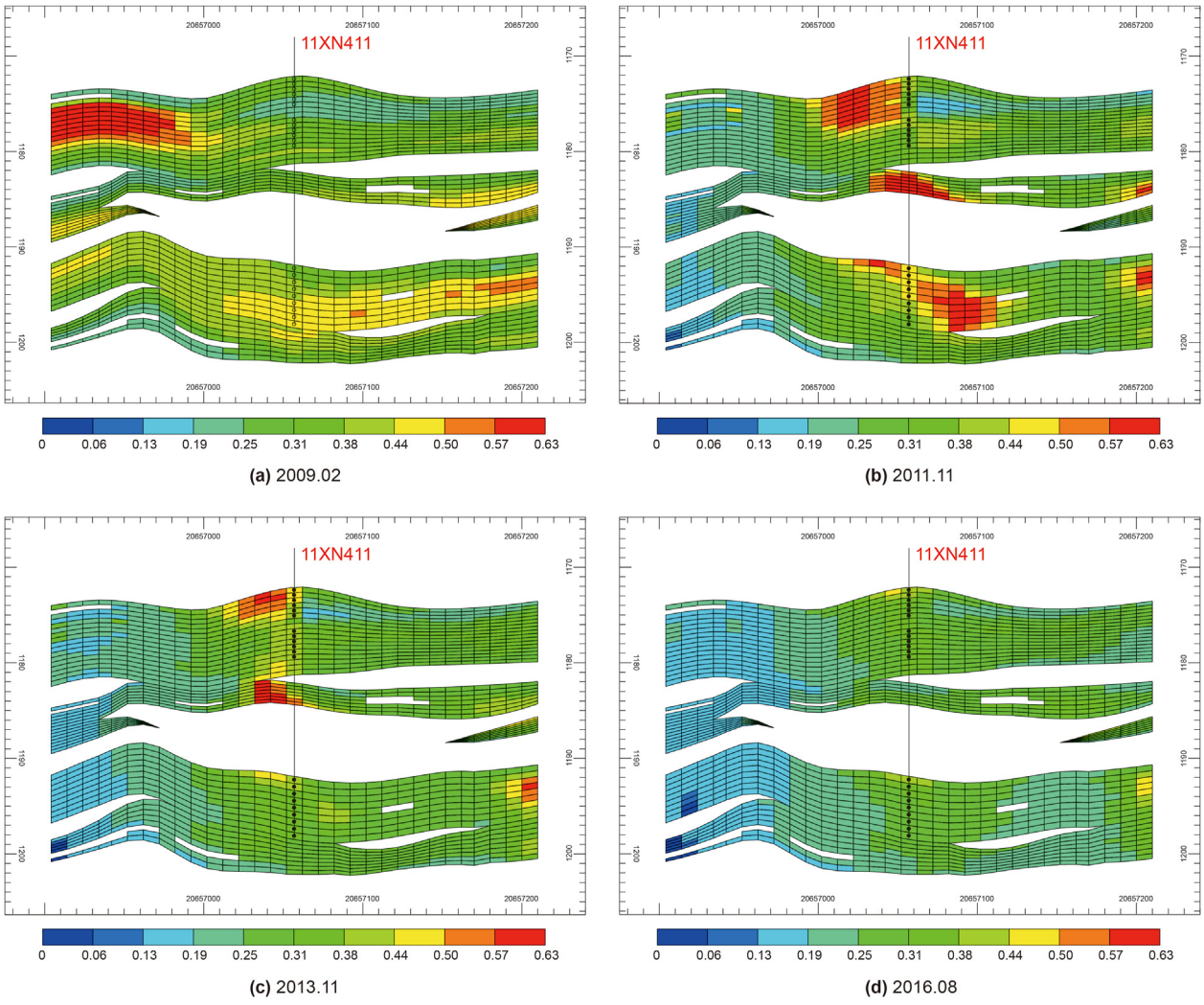

Fig. 6. Vertical distribution of remaining oil around producer 11XN411.

produced, the water cut increases by one step and remains relatively flat for several years. At this time, the sweep efficiency of the lower layers is obviously larger than that of the upper layers. Then, after the remaining oil displaced from the upper layers is completely produced, the water cut increases by another step, and the sweep efficiency of the upper layers reaches the similar level as that of the lower layers by the end of production. According to the sweep efficiency and pore volume in different layers in Fig. 7, the overall sweep efficiency can be calculated by pore volume weighted. The overall sweep efficiencies of layers 1–14, 35–41, and the whole perforating layers in Feburary 2009 are 0.84, 0.79, and 0.81. After infilling polymer-surfactant-PPG flooding, the overall sweep efficiencies increase to 0.90, 0.95, and 0.93 in June 2020, achieving effective sweep and production of the remaining oil after polymer flooding.

3.1.2. Gradual-decreasing W-type response

There are two reasons for gradual-decreasing W-type response according to the remaining oil distribution at different times in the numerical simulation. Firstly, the production well is located in areas with high remaining oil saturation after polymer flooding. Secondly, the remaining oil in other areas is displaced to the production well after infilling polymer-surfactant-PPG flooding, which achieves the second decrease of water cut. Taking producer 10X3010 as an example, Figs. 8–10 show the water cut curve, the vertical distribution of remaining oil at 4 time points, and the sweep efficiency of perforating layers at 3 time points, respectively. From Figs. 8–10, it can be seen that producer 10X3010 is put into production in June 2010, and the water cut is relatively low since the high remaining oil saturation around producer. Then, the remaining oil saturation around producer decreases and the sweep efficiency increases with the development, and thus the first decrease of water cut from 88.8% to 66.5% occurs in September 2011. After infilling polymer-surfactant-PPG flooding, there is a high oil saturation area on the right side of the producer, which greatly supplements the oil saturation around it. The sweep efficiency of each perforating layer is greatly increased, and the water cut further decreases to 33.6% in September 2012. After that, the water cut gradually rises with the production of the displaced remaining oil. By the end of July 2014, the displaced remaining oil has been largely produced as shown in Fig. 9(c and d). At this time, the water cut increases close to 100%, and the sweep efficiency of each perforating layer is nearly 30% higher than that before infilling polymer-surfactant-PPG flooding. It can be seen from Fig. 10 that the sweep efficiency after polymer flooding is generally low, and the overall sweep coefficient in perforating layers is only 0.55. After infilling polymer-surfactant-PPG flooding, it firstly increases to 0.69, and then to 0.89 in July 2014.

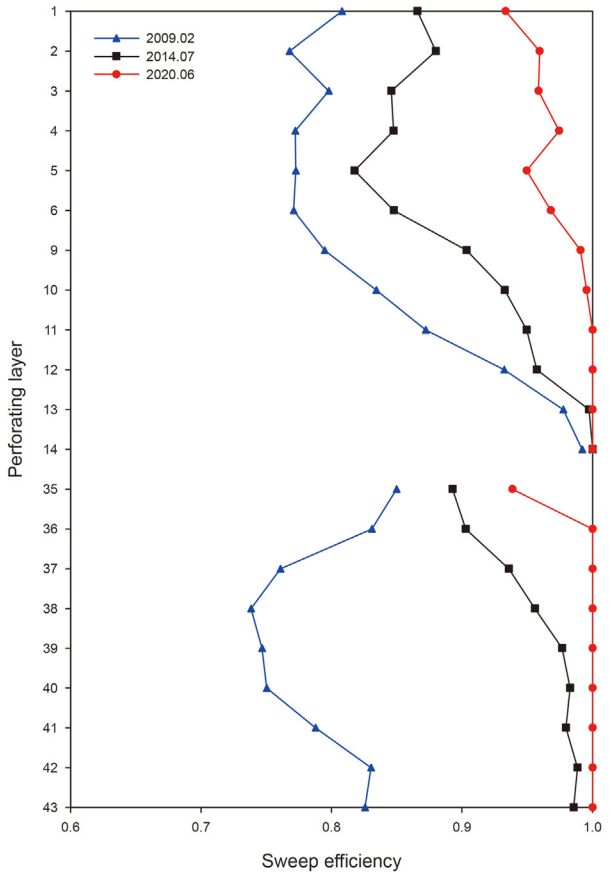

Fig. 7. Sweep efficiency of perforating layers around producer 11XN411.

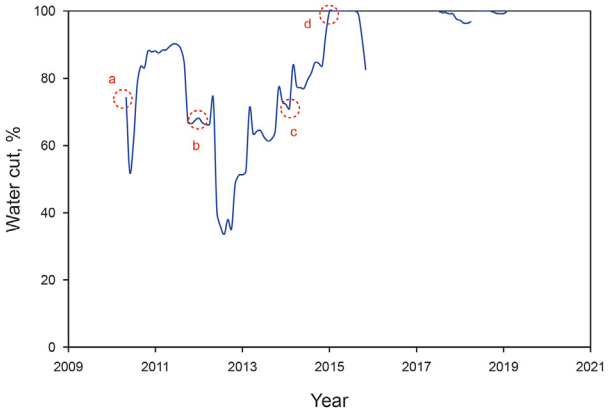

Fig. 8. Water cut curve of producer 10X3010.

3.2. U-type response

There are two reasons for U-type response according to the remaining oil distribution at different times in the numerical simulation. Firstly, narrow belts with high oil saturation are formed and displaced to the production well after infilling polymer-surfactant-PPG flooding. Secondly, high saturation oil belts in different directions synchronously are reached and produced within a short time, forming a deep and narrow water funnel. Taking producer 12X3012 as an example, Fig. 11 shows the water cut curve, and Fig. 12 shows the horizontal distribution of remaining oil at 4 time points in the 37th layer of the model. From Figs. 11 and 12, it can be seen that the original remaining oil saturation around it is relatively high after polymer flooding, and the water cut firstly decreases and then increases after it is opened in July 2010. After well pattern infilling, the infilled injectors 12X3312 and 13X3312 are located in the high remaining oil saturation area, and narrow belts with high oil saturation are formed and displaced to the producer 12X3012 together with polymer-surfactant-PPG flooding. In October 2011, the oil belts are synchronously displaced to the production well, and the water cut decreases rapidly to 31.7% and remains flat. Then, the water cut rises rapidly due to insufficient replenishment of remaining oil after developing in a low water cut stage for about 1 year. Fig. 13 shows the changes in oil saturation and seepage resistance along the connection line between injector 12X3312 and producer 12X3012 in the 37th layer. The abscissa represents the number of grids from injector 12X3312. Specifically, 0 represents injector 12X3312 and 14 represents producer 12X3012. Moreover, the curve and column in the figure represent the seepage resistance and oil saturation, respectively. It can be seen from the figure that the maximum seepage resistance increases by nearly 8 times after polymer-surfactant-PPG flooding, which is mainly caused by two reasons. On the one hand, the viscosity of the water phase increases due to the injection of polymer. On the other hand, the injection of PPG can plug water channeling regions, resulting in a decrease in the absolute permeability of water channeling regions and promoting the transfer of the injected fluid to the oil enriched area. Furthermore, the concentration of polymer and PPG in displacing fluid after oil belts is relatively high, so the seepage resistance is the largest in front of the displacing fluid. In addition, the remaining oil gathers before the front of the displacing fluid and forms higher saturation oil belts, so the seepage resistance of oil belts in front of the seepage resistance peak of the displacing fluid is higher than that of the unswept area by polymer-surfactant-PPG flooding. Furthermore, the peak value of seepage resistance is similar, which is 0.0374, 0.0358, 0.0319, and 0.0325, in August 2010, November 2010, November 2011, and September 2012, respectively. And the sum of seepage resistance along the connection line gradually increases with time, which are 0.0994, 0.1407, 0.2030, and 0.2425, respectively. With the development of polymer-surfactant-PPG flooding, narrow belts with high oil saturation are enriched continuously and gradually displaced to producer 12X3012.

3.3. V-type response

3.3.1. Early V-type response

According to the remaining oil distribution at different times in the numerical simulation, the main reason for early V-type response is that the infilled production well is located in the area with high remaining oil saturation after polymer flooding, and the remaining oil is quickly produced after the production well is opened. Additionally, the amount of remaining oil of early V-type response is not much enough to maintain a longer stage of low water cut, which is different from U-type response. Taking producer 12X3013 as an example, Figs. 14–16 show the water cut curve, the vertical distribution of remaining oil at 4 time points, and the sweep efficiency of perforating layers at 3 time points, respectively. As can be seen from these figures, infilled producer 12X3013 is put into production in July 2010, and the water cut decreases to 86.3% rapidly due to the high remaining oil saturation. However, since the amount of remaining oil is small, the water cut rises rapidly and cannot form a longer production stage with low water cut similar to U-type response. Besides, the remaining oil in other areas is gradually displaced to the production well after the injection of polymer-surfactant-PPG system, so the water cut shows a second decline. After that, the water cut quickly increases to

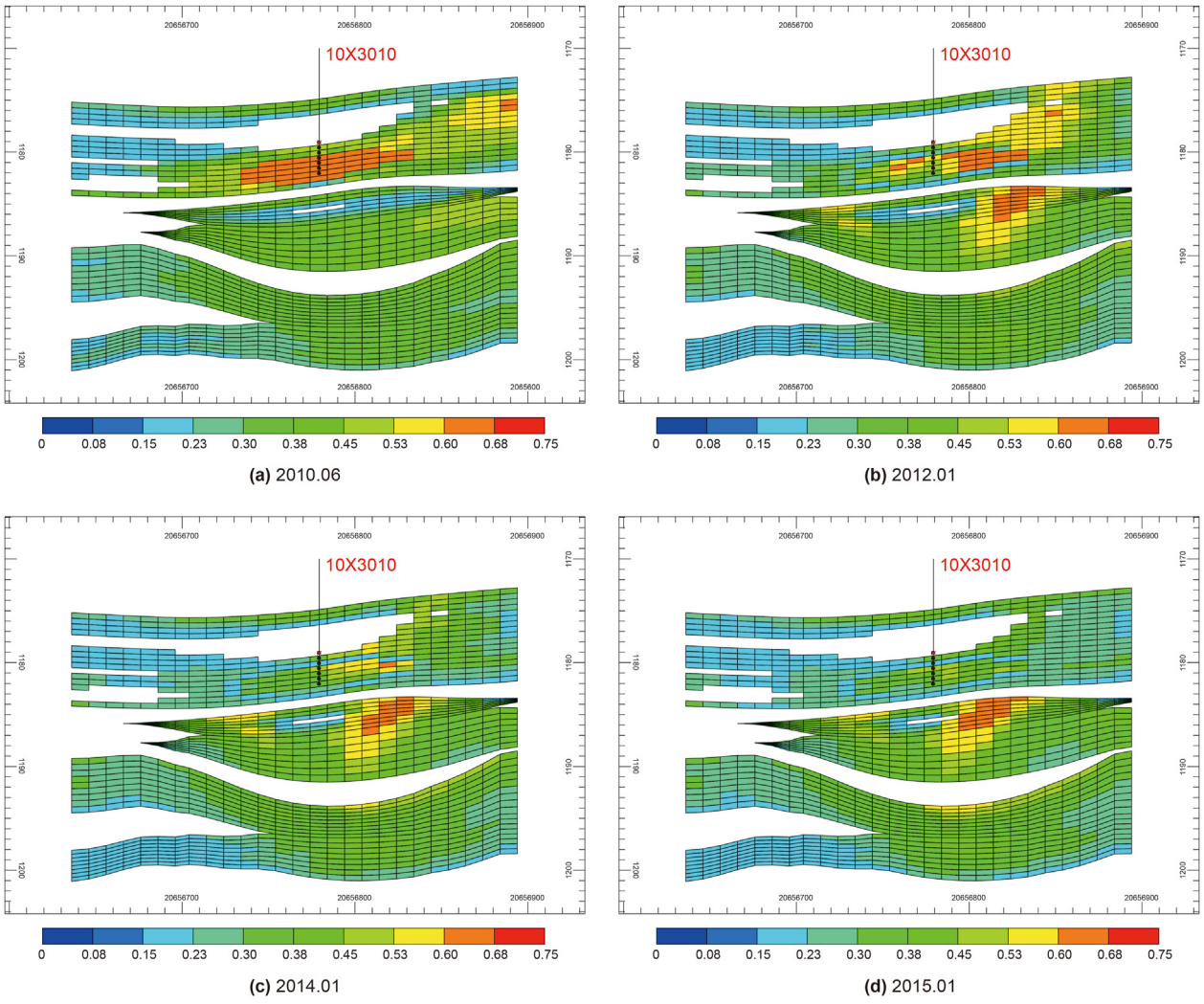

Fig. 9. Vertical distribution of remaining oil around producer 10X3010.

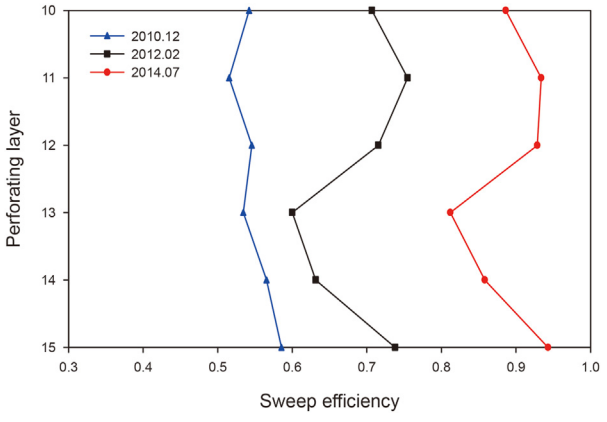

Fig. 10. Sweep efficiency of perforating layers around producer 10X3010.

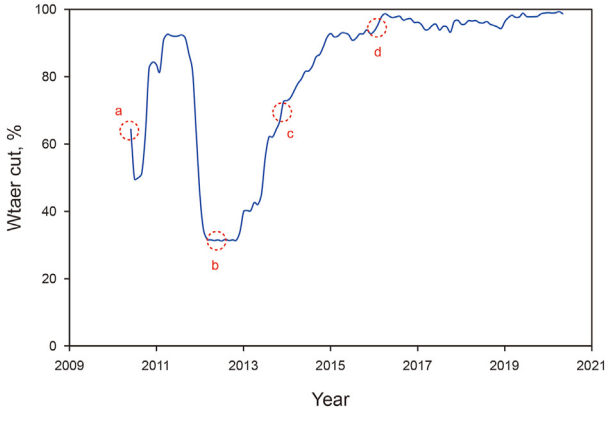

Fig. 11. Water cut curve of producer 12X3012.

nearly 100% and then the well is shut-in in October 2014. Noticeably, the characteristics of this type different from delayed V-type response is the first decrease of response. Moreover, the difference between this type and gradual-decreasing W-type response is that the remaining oil around the infilled producer has been completely produced before the remaining oil is displaced from other areas reaching the well. It can be seen from Fig. 16 that the sweep efficiency is generally high before infilling polymer-surfactant-PPG flooding, and only layers 39–43 are low. The overall sweep efficiencies of layers 1–12 and 35–43 are 0.95 and 0.92, and 0.94 in the

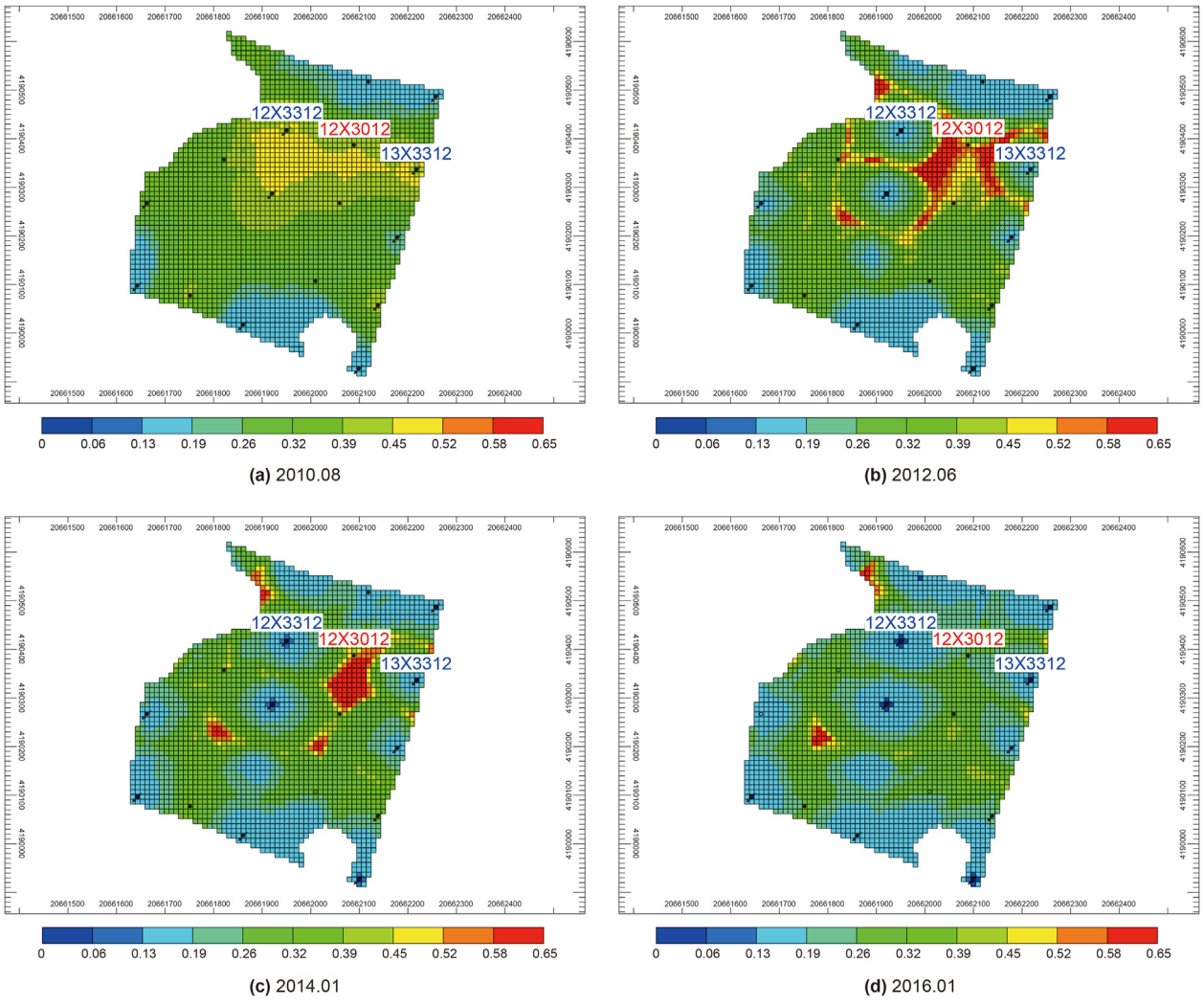

Fig. 12. Horizontal distribution of remaining oil in the 37th layer of the model.

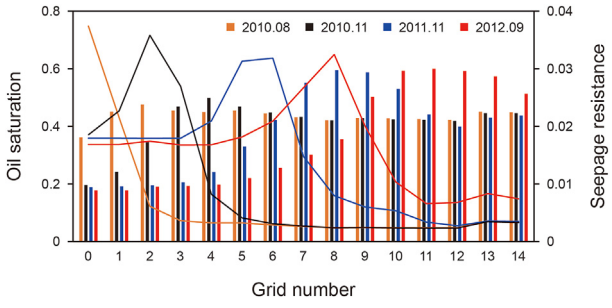

Fig. 13. Oil saturation and seepage resistance along the connection line between injector 12X3312 and producer 12X3012.

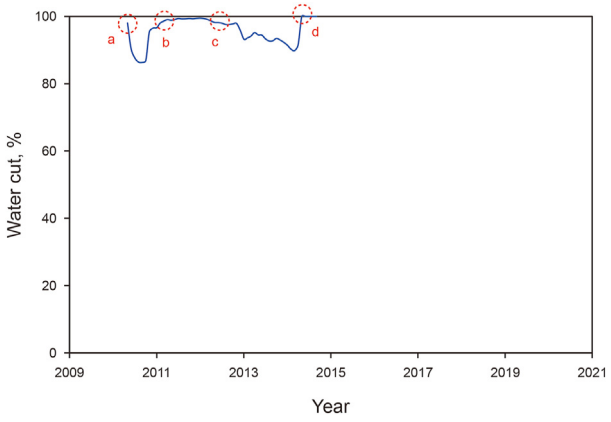

Fig. 14. Water cut curve of producer 12X3013.

whole perforating layers. From Fig. 15(a), it can also be seen that the remaining oil saturation in these layers is generally high. After infilling polymer-surfactant-PPG flooding in July 2014, the overall swept efficiency is nearly 1, and each layer is almost completely swept when the well is shut-in.

3.3.2. Delayed V-type response

According to the remaining oil distribution at different times in the numerical simulation, the main reason for delayed V-type response is that the original production well is located in the area with low remaining oil saturation after polymer flooding, resulting in no significant decrease in water cut for a long time after the production well is opened. Additionally, it takes a long time to displace the remaining oil from other areas to the production well

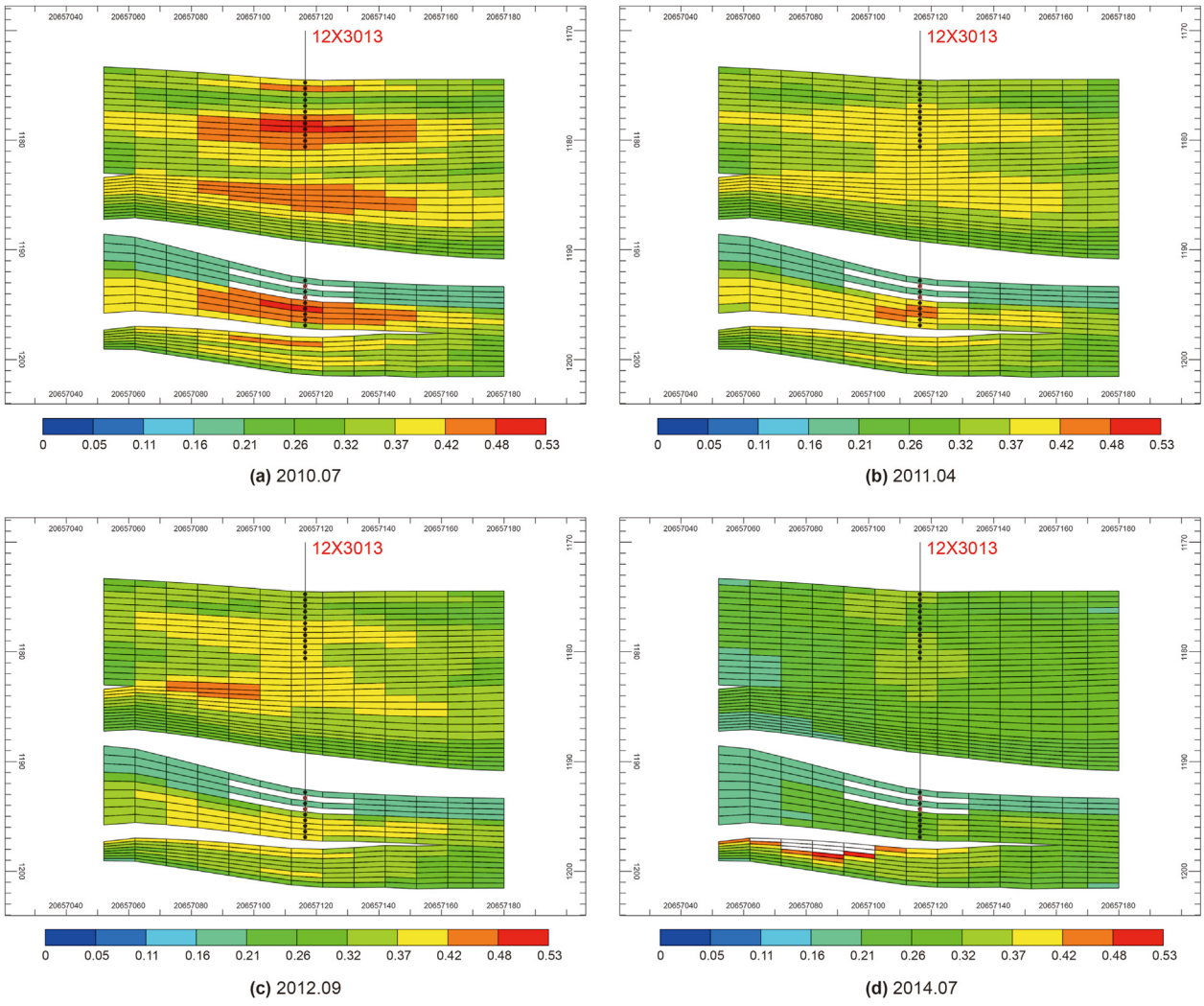

Fig. 15. Vertical distribution of remaining oil around producer 12X3013.

after polymer-surfactant-PPG flooding. Taking producer 11J11 as an example, Fig. 17 shows the water cut curve, and Fig. 18 shows the horizontal distribution of remaining oil at 4 time points in the 30th layer of the model. From Figs. 17 and 18, it can be seen that the water cut maintains a high level because producer 11J11 is an original producer and the remaining oil saturation around it after polymer flooding is low. After infilling polymer-surfactant-PPG flooding, the remaining oil in different directions is gradually displaced to it and the water cut decreases rapidly to 64.8% in April 2012. Subsequently, the water cut gradually increases with the production of the displaced remaining oil, and the well is shut-in when the water cut reaches 100% in November 2014. Fig. 19 shows the changes in oil saturation and seepage resistance along the connection line between injector 11X3311 and producer 11J11 in the 30th layer. The abscissa represents the number of grids from injector 11X3311. Specifically, 0 represents the injector 11X3311 and 10 represents the producer 11J11. The curve and column in the figure represent the seepage resistance and oil saturation, respectively. Similar to Fig. 13, the seepage resistance of injector 11X3311 increases significantly after polymer-surfactant-PPG flooding. Meanwhile, a high oil saturation area is formed in front of the seepage resistance peak and gradually displaced to producer 11J11. The difference is that the seepage resistance along the connection line between injector 11X3311 and producer 11J11 is relatively smaller as a whole compared with U-type response, and the peak value of seepage resistance is 0.0271, 0.0295, and 0.0243. Moreover, the sum of seepage resistance along the connection line is 0.0677, 0.1486, and 0.1654, respectively.

3.4. No response

There are two reasons for no response according to the remaining oil distribution at different times in the numerical simulation. Firstly, the remaining oil saturation after polymer flooding around the production well is low. Secondly, the remaining oil displaced from other areas can not be effectively produced before the production well is shut-in after infilling polymer-surfactant-PPG flooding. Taking producer 11X3010 as an example, Fig. 20 shows the water cut curve, and Fig. 21 shows the horizontal distribution of remaining oil at 4 time points in the 1st layer of the model. As can be seen from these figures, producer 11X3010 is opened in July 2010. And there is no significant decrease in water cut due to the low remaining oil saturation around it. At the same time, it is shut-in in March 2013 before the remaining oil is displaced to it because of its high water cut of over 99% for a long time. Therefore, there is no significant decrease in water cut during the development process of infilling polymer-surfactant-PPG flooding, which is a no response type.

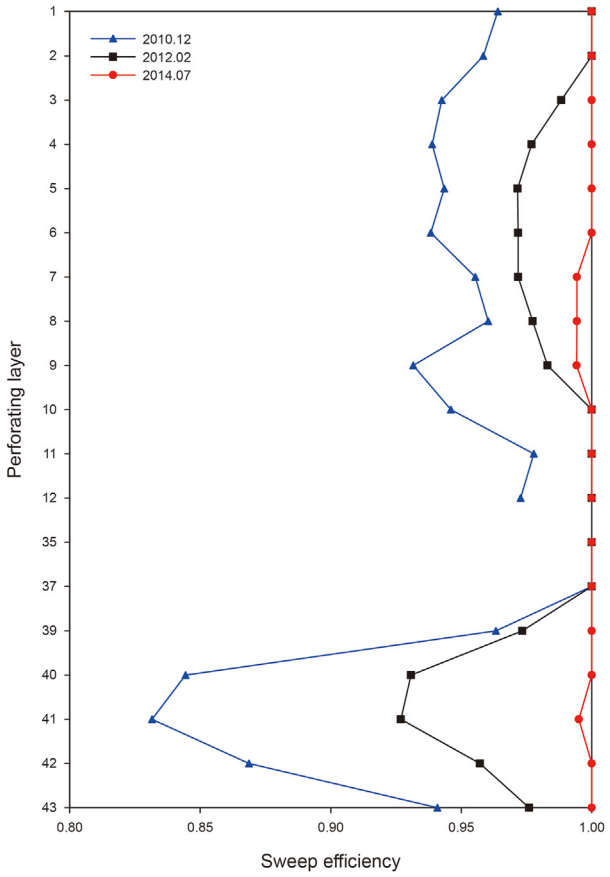

Fig. 16. Sweep efficiency of perforating layers around producer 12X3013.

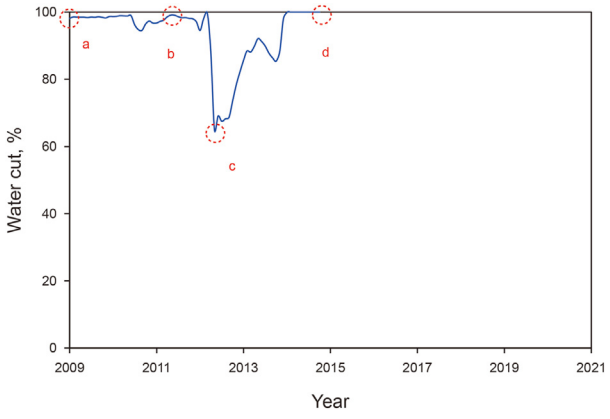

Fig. 17. Water cut curve of producer 11J11.

4. Remaining oil distribution and displacement mechanisms

4.1. Remaining oil distribution after polymer flooding

Based on reservoir numerical simulations, the research on the remaining oil distribution after polymer flooding is carried out in combination with field production data and test data. Generally, there is still a large amount of remaining oil after polymer flooding, which is characterized by widespread distribution and local enrichment in the non-mainstream line area (Du et al., 2019; Wu et al., 2020). According to previous studies, the distribution characteristics of remaining oil after polymer flooding are similar in each layer separated by interlayers under the influence of interlayers (Hou et al., 2011). Moreover, the remaining oil is enriched at the top of the positive rhythm layer, and the closer it is to the production well, the more abundant the remaining oil is (Hou et al., 2010). Based on the above studies and geological characteristics in the pilot test, the remaining oil after polymer flooding can be divided into four types of distribution as shown in Fig. 22, including disconnected remaining oil, streamline unswept remaining oil, rhythm remaining oil, and interlayer-controlled remaining oil. It can be seen from the figure that the disconnected remaining oil is characterized by the local enrichment of remaining oil due to the incomplete geological structure and injection-production relationship, such as the lower right area of producer 11J11. The injection-production relationship of streamline unswept remaining oil is relatively complete. However, the injected fluid flows in the direction of low seepage resistance due to the existence of water channeling regions formed during water flooding and polymer flooding, resulting in the local enrichment of remaining oil, such as the area around producer 11XN411. The characteristics of rhythm remaining oil include interlayer heterogeneity and intralayer rhythm. The interlayer heterogeneity shows the high remaining oil saturation in the upper part of the reservoir while low in the lower part, reflecting the channeling phenomenon of displacement fluid along the lower part. The intralayer rhythm is characterized by the enrichment of remaining oil at the top of each layer, reflecting the flow of displacement fluid along the bottom of the layer. This phenomenon is especially evident in layers with high remaining oil saturation. The characteristic of interlayer-controlled remaining oil is that there is a lot of remaining oil in the low permeability area in each layer. As shown around producer 12X3013, the remaining oil is enriched in each layer that the well passes through.

4.2. Displacement mechanisms of infilling polymer-surfactant-PPG flooding

The addition of PPG to the polymer-surfactant system can show a stronger ability to increase flow resistance and profile control. It tends to flow along the water channeling regions during the injection process. When it flows to the pore throat, the flow resistance at the flow front increases because of particle retention and compressional deformation, which is reflected as an increase in displacement pressure difference It can deform and pass through the pore throat under the action of displacement pressure difference when it is greater than the extrusion pressure. However, when the displacement pressure difference is not large enough to allow it to deform and pass through the pore throat, it stays to plug the water channeling regions and divert the subsequent displacement fluid, which realizes the profile control (Zhou et al., 2018, 2019).

Since it is difficult to count the displacement pressure difference of each grid in the numerical simulation model, the dimensionless seepage resistance is used to characterize the displacement pressure difference according to Darcy's law. The remaining oil saturation field and dimensionless seepage resistance field are used to analyze the displacement mechanisms of disconnected remaining oil and streamline unswept remaining oil. The profile control is characterized by the water absorption profile before and after infilling polymer-surfactant-PPG flooding, and it is used to analyze rhythmic remaining oil and interlayer-controlled remaining oil in combination with remaining oil distribution.

(1) Dimensionless seepage resistance.

Since the polymer-surfactant-PPG system can not only increase the viscosity of water phase, but also reduce the permeability of water channeling regions by plugging pore throat, there is a large

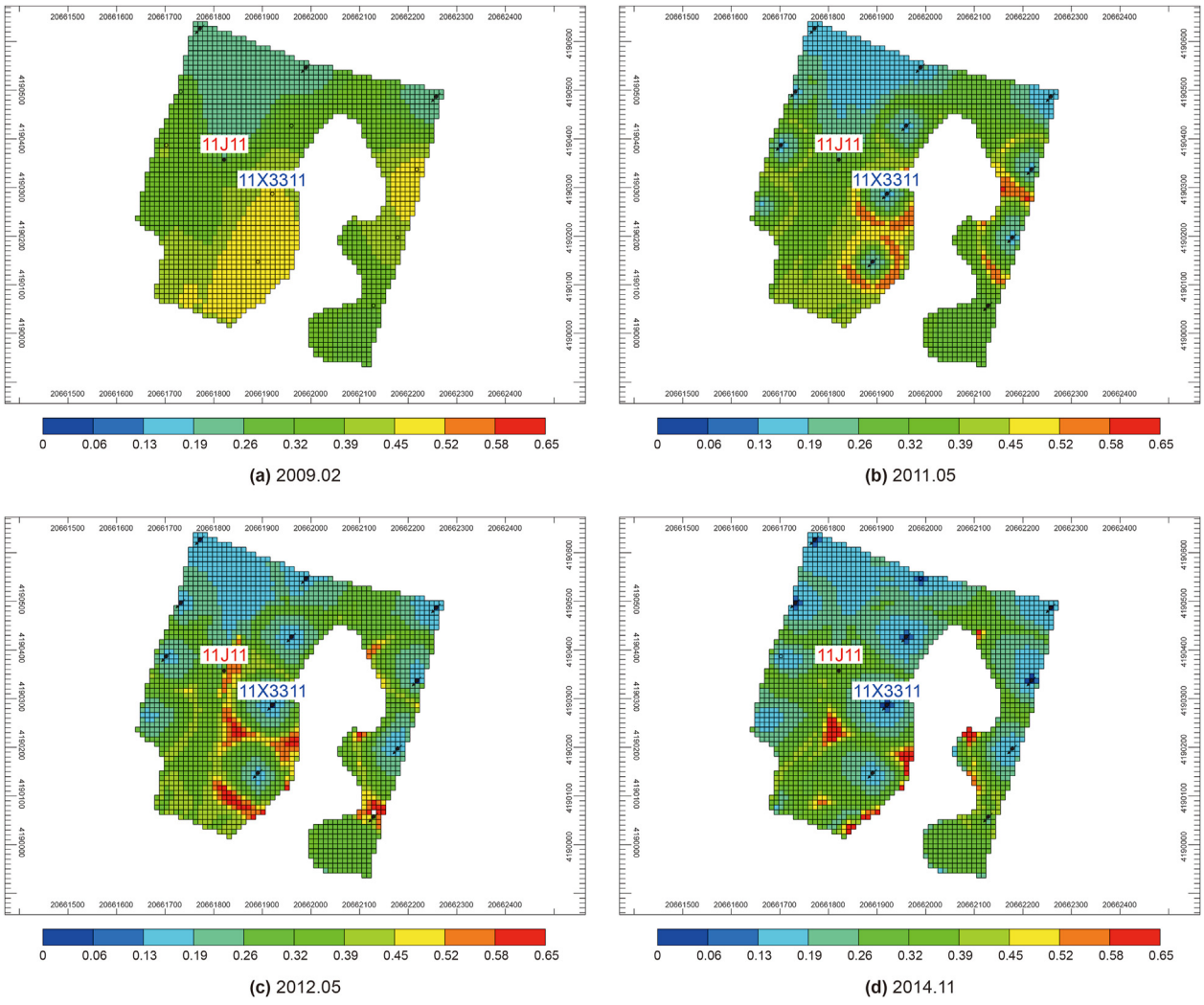

Fig. 18. Horizontal distribution of remaining oil in the 30th layer of the model.

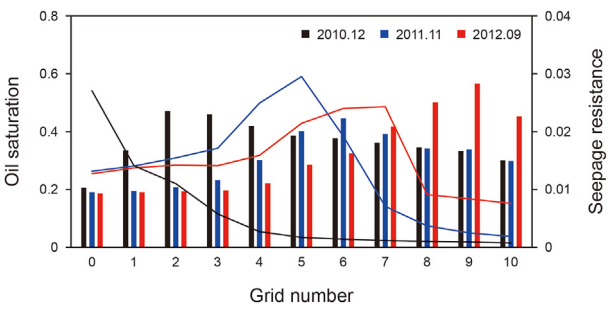

Fig. 19. Oil saturation and seepage resistance along the connection line between injector 11X3311 and producer 11J11.

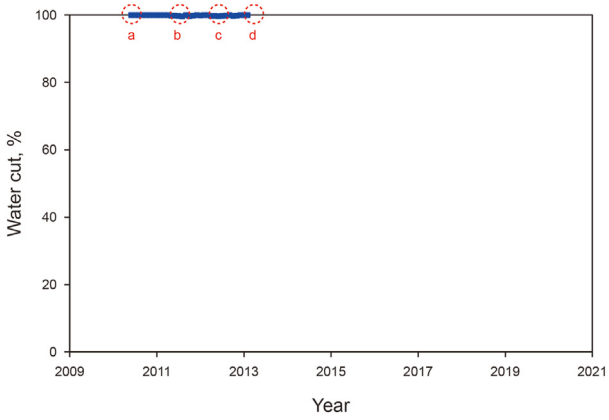

Fig. 20. Water cut curve of producer 11X3010.

order of magnitude difference in seepage resistance before and after infilling polymer-surfactant-PPG flooding. Therefore, the seepage resistance of each grid obtained by Eq. (1) is converted into dimensionless seepage resistance, which is convenient to characterize the relative change of seepage resistance. The calculation equation is shown in Eq. (6). The maximum and minimum seepage resistance are counted in the selected layer in the dimensionless process since the seepage resistance is only analyzed on the plane.

$$R_t^{i,j} = \frac{R^{i,j} - R_{\min}}{R_{\max} - R_{\min}} \tag{6}$$

where $R_t^{i,j}$ is the dimensionless seepage resistance of the grid (i,j); $R_{\max}$ and $R_{\min}$ are the maximum and minimum seepage resistance in the selected layer, respectively.

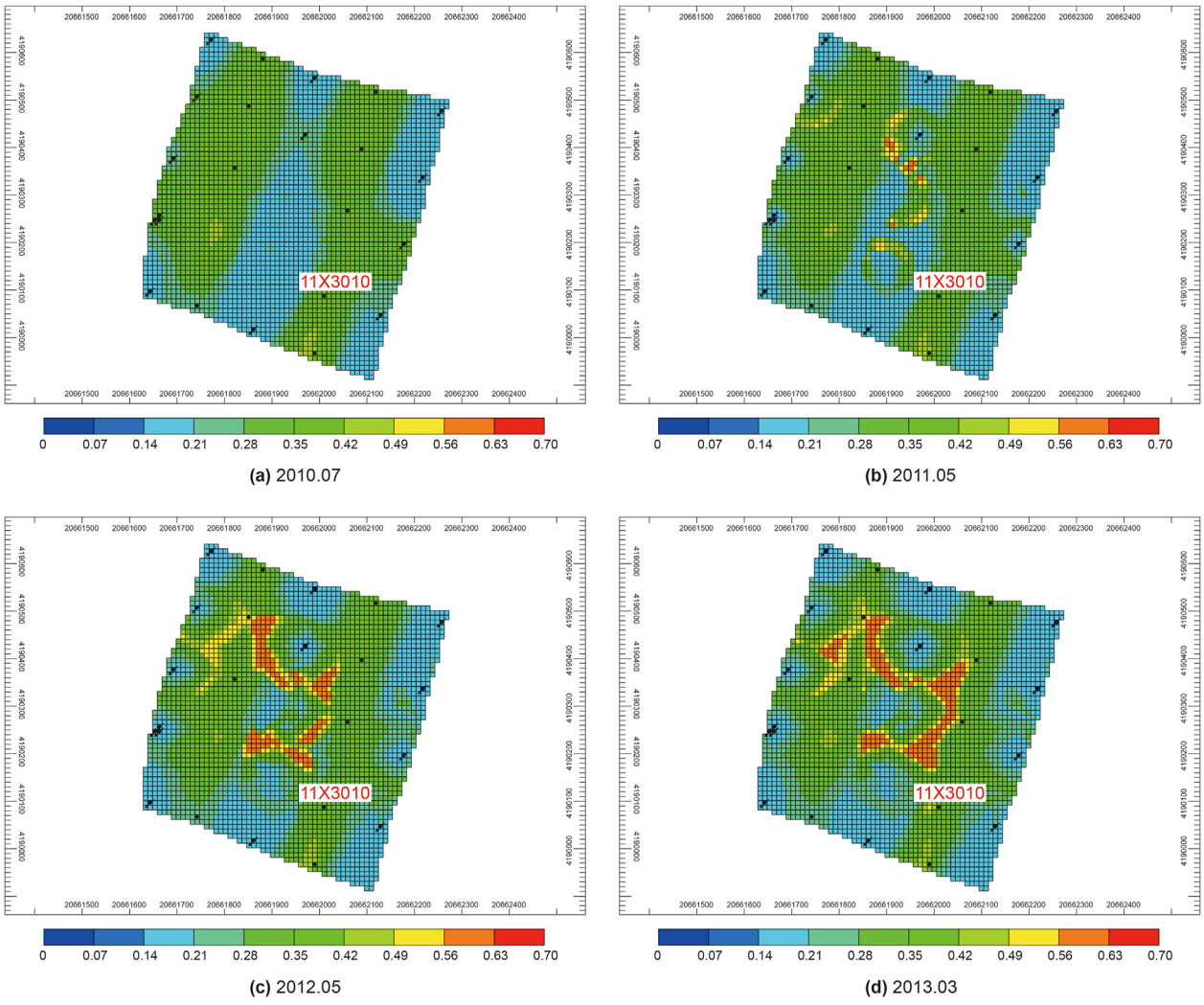

Fig. 21. Horizontal distribution of remaining oil in the 1st layer of the model.

(2) Water absorption profile.

As shown in Eq. (7), the proportion of the water absorption of each layer to the sum of all layers at two time points is firstly counted, and the difference of the proportion between two time points is calculated layer by layer. Then, the difference of the proportion is divided by the proportion at time point before infilling polymer-surfactant-PPG flooding in order to obtain the change of water absorption profile. Considering the early shut-in time of some production wells, time points selected in this paper are February 2009 and January 2016, which are the start time of simulation and the start time of subsequent water flooding, respectively. It is worth noting that different colors are used to represent layers separated by interlayers. In this paper, layers 1–17, 19–25, 27–33, 35–43, and 45–52 are shown in blue, red, black, green, and yellow, respectively.

$$W^k = \frac{\left(I^k_{ts} \Big/ \sum^n I^k_{ts}\right) - \left(I^k_{te} \Big/ \sum^n I^k_{te}\right)}{\left(I^k_{te} \Big/ \sum^n I^k_{te}\right)} \tag{7}$$

where W^k is the change of water absorption profile of layer k; I^k_{ts} and I^k_{te} are the proportion of water absorption of layer k of the injection well at time point ts and te; n is the number of perforating layers.

4.2.1. Disconnected remaining oil

Figs. 23 and 24 show the dimensionless seepage resistance field and the remaining oil saturation field in the disconnected remaining oil area. It can be seen that the remaining oil is enriched in the lower right area of producer 11J11 due to incomplete geological structure and injection-production relationship before infilling polymer-surfactant-PPG flooding. The infilled injector 11X3310 and producer 9X3009 are drilled in the disconnected remaining oil enrichment area before polymer-surfactant-PPG flooding. The well pattern infilling changes the original injection-production relationship, which can guide polymer-surfactant-PPG system to the remaining oil enrichment area and give full play to its role (Du et al., 2019; Wu et al., 2020). At the same time, the dimensionless seepage resistance near the injector increases significantly with the injection of polymer-surfactant-PPG system because of the viscosity increasing effect of polymer and plugging effect of PPG. On the one hand, the injected fluid pushes the remaining oil toward the producer. On the other hand, the injected fluid tends to flow along the unswept area with high remaining oil saturation between two injectors, since the seepage resistance in

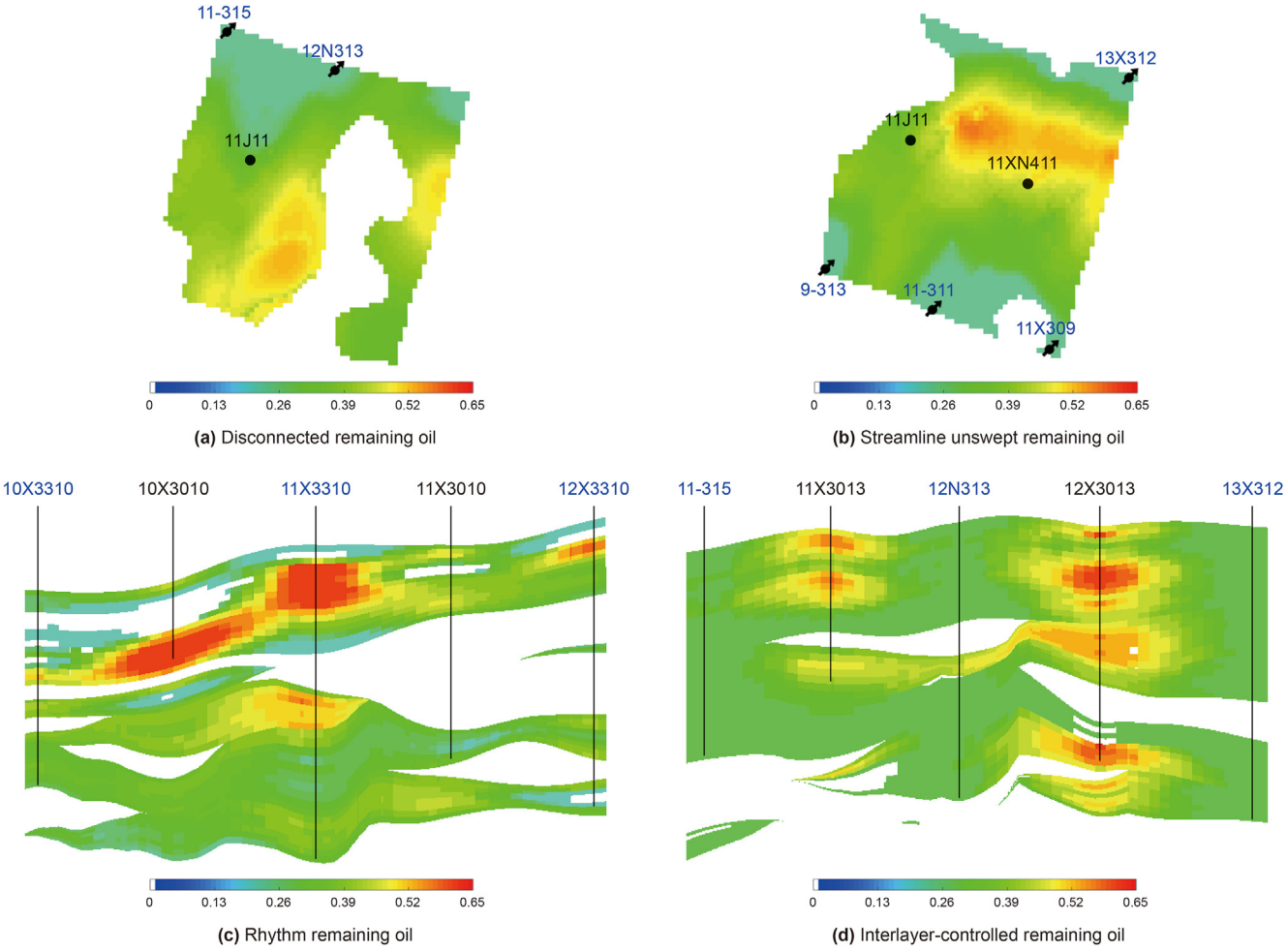

Fig. 22. Four types of remaining oil distribution.

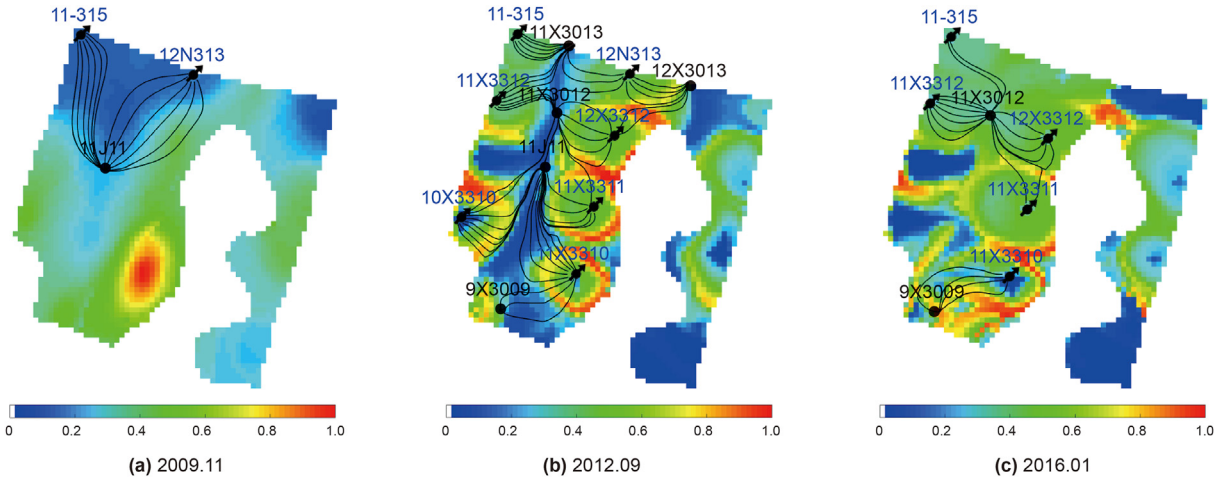

Fig. 23. Dimensionless seepage resistance and streamline in the disconnected remaining oil area.

unswept area is relatively small. As shown in Figs. 23(b) and 24(b), the remaining oil is displaced to producers 9X3009 and 11J11, and effectively produced. Combined with the previous study of production characteristics, producers 9X3009 and 11J11 respectively show early V-type and delayed V-type response, which is probably the response of this type of remaining oil distribution. The difference results from the amount of remaining oil around producer after polymer flooding.

4.2.2. Streamline unswept remaining oil

Figs. 25 and 26 show the dimensionless seepage resistance field and the remaining oil saturation field in the streamline unswept

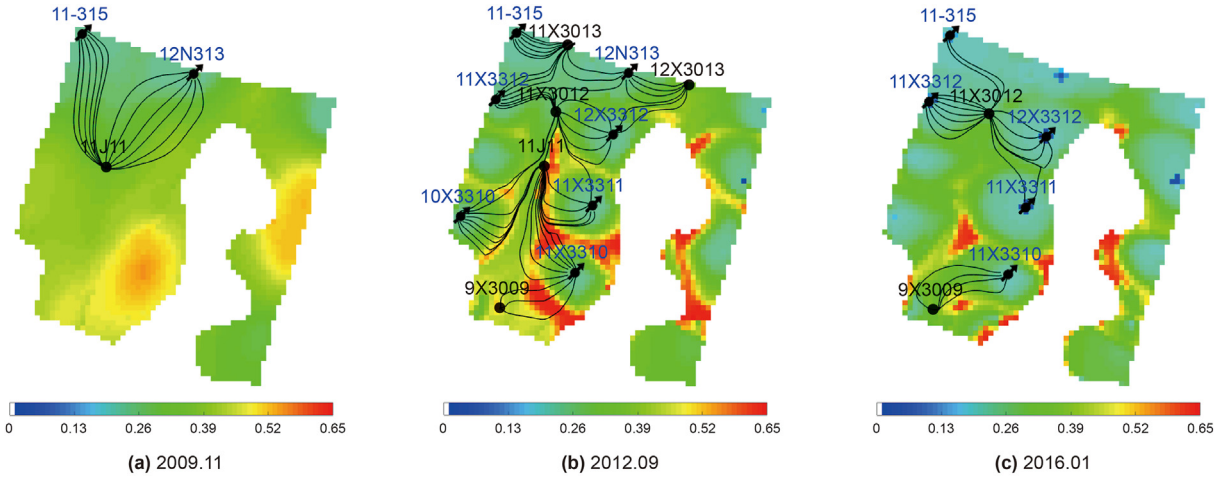

Fig. 24. Remaining oil saturation and streamline in the disconnected remaining oil area.

remaining oil area. As can be seen from these figures, the injected fluid of injector 13X312 flows along the area of low seepage resistance before infilling polymer-surfactant-PPG flooding, resulting in the low sweep efficiency and a large amount of remaining oil in the unswept area. After that, infilled injectors 12X3312, 13X3312, and producer 12X3012 are drilled in the unswept area, which changes the original direction of the main streamline between injection and production wells and expands the swept area of injected fluid (Du et al., 2019; Wu et al., 2020). Meanwhile, the injection of polymer-surfactant-PPG system adjusts the distribution of the seepage resistance field because of the viscosity increasing effect of polymer and plugging effect of PPG, and the injected fluid is diverted to the remaining oil enrichment area with low seepage resistance. Therefore, the streamline unswept remaining oil realizes effectively produced. Combined with the previous study of production characteristics, producers 11XN411 and 12X3012 respectively show U-type and gradual-rising W-type response, which is resulting from the amount of this type of remaining oil around producer and the reaching time of remaining oil displaced from other areas.

4.2.3. Rhythm remaining oil

Fig. 27 shows the changes in the remaining oil distribution and water absorption profile in the rhythmic remaining oil area. Noticeably, the separated layer water injection has been conducted before infilling polymer-surfactant-PPG flooding. It is separated into layers 1–28 and 35–43 for injector 10X3310, and layers 3–33 and 39–52 for injector 11X3310. From Fig. 27(a and b), it can be seen that the remaining oil is enriched in the upper part of the reservoir and the top of each layer due to interlayer heterogeneity and intralayer rhythm, while it is effectively produced after infilling polymer-surfactant-PPG flooding. After the injection of polymer-surfactant-PPG system, it firstly tends to flow along the water channeling regions with low remaining oil saturation. When large amounts of PPGs are injected to the water channeling regions, their plugging effects are superimposed, forcing the subsequent injection fluid to divert to the low permeable regions with high remaining oil saturation. Therefore, it can achieve profile control effect (Zhou et al., 2019). As can be seen from Fig. 27(c and d), the water absorption of layers 1–28 of injector 10X3310 increases as a whole after infilling polymer-surfactant-PPG flooding, especially the proportion of water absorption of layers 11–17 enriched with remaining oil is increased by 889.59%. For injector 11X3310, the injection of polymer-surfactant-PPG system plugs water channeling regions, which is reflected as a decrease in water absorption in the layer with low oil saturation while an increase in the layer with high oil saturation. As shown in Fig. 27(d), the proportion of water absorption of layers 4–10 and 27–33 increases by 1667.02% and 1501.60%, respectively. Therefore, the remaining oil in the

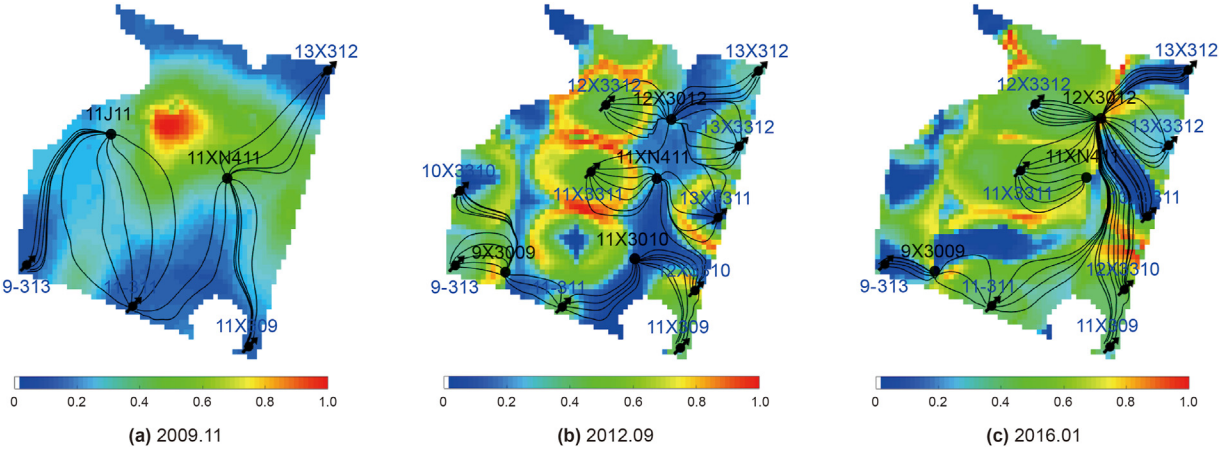

Fig. 25. Dimensionless seepage resistance and streamline in the disconnected remaining oil area.

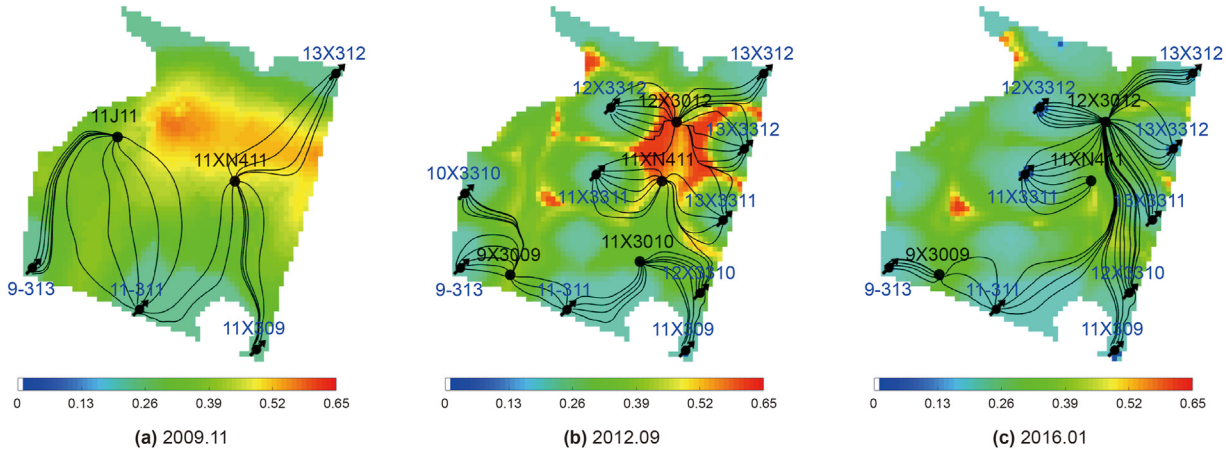

Fig. 26. Remaining oil saturation and streamline in the disconnected remaining oil area.

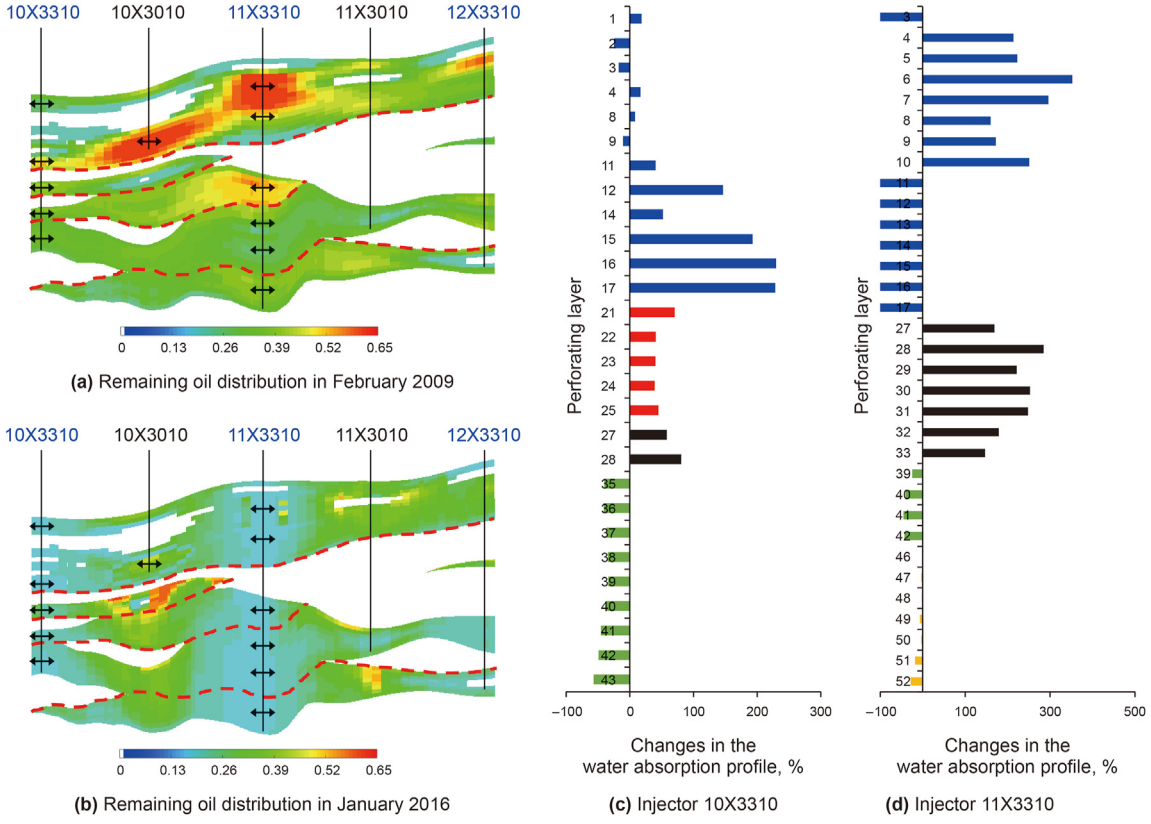

Fig. 27. Remaining oil distribution and water absorption profile change in the rhythmic remaining oil area.

unswept area or low-swept area can be effectively displaced and produced. Combined with the previous study of production characteristics, producer 10X3010 shows gradual-decreasing W-type response, which is probably the response of this type of remaining oil distribution.

4.2.4. Interlayer-controlled remaining oil

Fig. 28 shows the changes in the remaining oil distribution and water absorption profile in the interlayer-controlled remaining oil area. Noticeably, the separated layer water injection has been conducted before infilling polymer-surfactant-PPG flooding. It is separated into layers 1–30 and 39–43 for injector 12N313, and layers 1–33 and 36–52 for injector 13X312. From Fig. 28(a and b), it can be seen that there is a lot of remaining oil in each layer since the producer is located in the non-mainstream line area and controlled by the interlayer, which is effectively displaced by infilling polymer-surfactant-PPG flooding. For injector 12N313, the water absorption of layers 1–11 and 19–25 with remaining oil enrichment on both sides increases significantly because of the profile control of polymer-surfactant-PPG system, and basically shows a decreasing trend from top to bottom (Zhou et al., 2019). Based on Fig. 28(c), the proportion of water absorption layers of 1–8 and 19–25 increases by 560.47% and 193.64%. However, layers 39–43 controlled by geological structure are only enriched with remaining oil on one

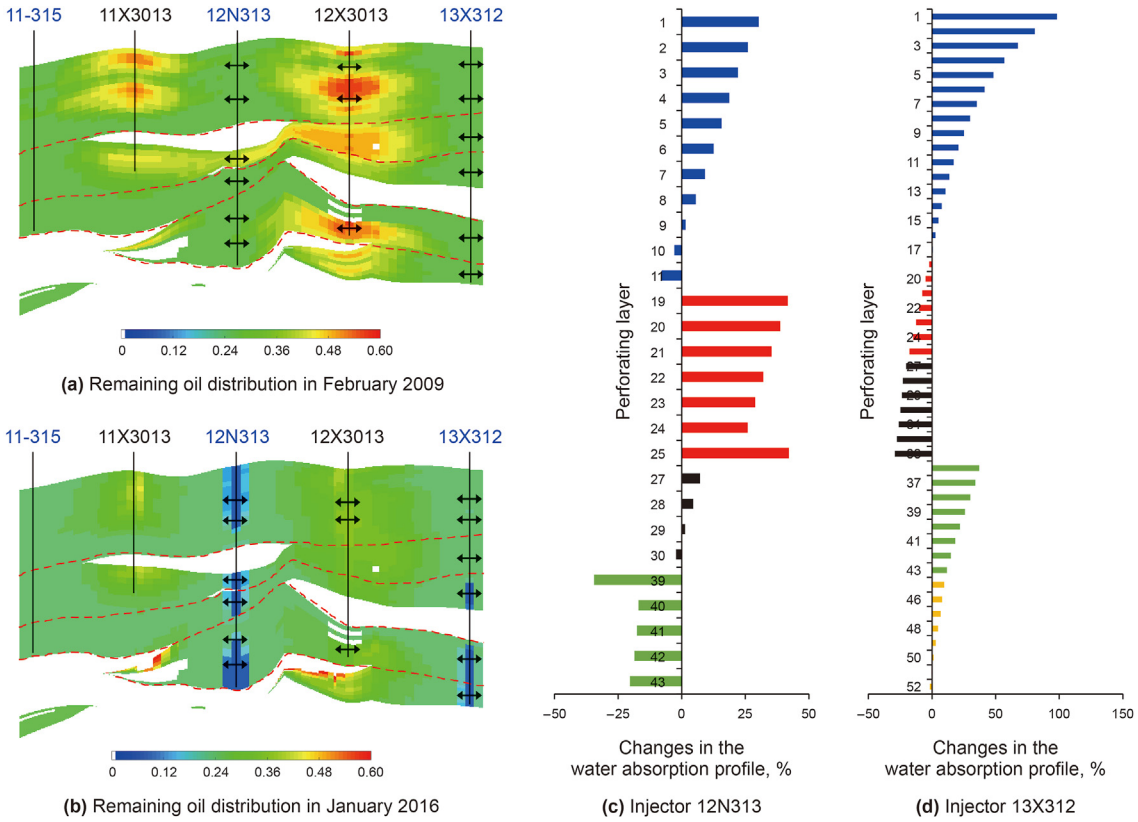

Fig. 28. Remaining oil distribution and water absorption profile change in the interlayer-controlled remaining oil area.

side, and the water absorption is generally reduced. Besides, the water absorption of layers 1–18 and 35–43 of injector 13X312 increases as a whole and also decreases from top to bottom because producer 12X3013 with perforating layers 1–18 and 35–43 is the only directly effective well. And the proportion of water absorption of layers 1–17 and 35–43 increases by 560.47% and 193.64%. Combined with the previous study of production characteristics, producer 12X3013 show early V-type response, which is probably the response of this type of remaining oil distribution.

5. Conclusions

Based on the production and test data of the pilot test in Ng3 block of Gudao Oilfield, this paper analyzes the production characteristics and displacement mechanisms of infilling polymer-surfactant-PPG flooding for post-polymer flooding reservoir. The underlying reasons of production characteristics are analyzed by seepage resistance and sweep efficiency, and displacement mechanisms are clarified by dimensionless seepage resistance and water absorption profile. Finally, the production characteristics of different types of remaining oil distribution after infilling polymer-surfactant-PPG flooding are summarized. The following conclusions can be drawn in detail.

(1) Production characteristics after infilling polymer-surfactant-PPG flooding include W-type, U-type, V-type response, and no response. Specifically, the W-type response is further subdivided into gradual-rising W-type and gradual-decreasing W-type. The V-type response is further subdivided into early V-type and delayed V-type. When the production well is located in the area enriched with remaining oil after polymer flooding and there is also remaining oil displaced from other areas by polymer-surfactant-PPG flooding, the producer will show early V-type response or gradual-decreasing W-type response depending on the reaching time of remaining oil in different areas are the same or not. When the production well is located in the area with low remaining oil saturation after polymer flooding and the saturation of oil belts formed by polymer-surfactant-PPG flooding is low, the production well will show delayed V-type response. Otherwise for high saturation oil belts, the production well will show U-type response or gradual-rising W-type response according to the production end time of oil belts in different directions are the same or not. In particular, it will show no response if the production well is shut-in before the reach of displaced remaining oil.

(2) Remaining oil distributions after polymer flooding include disconnected remaining oil, streamline unswept remaining oil, rhythm remaining oil, and interlayer-controlled remaining oil. Taking the development of the pilot test as an example, the production of disconnected remaining oil needs the improvement of injection-production connectivity by well pattern infilling, and usually shows V-type response. The recovery of streamline unswept remaining oil enhances due to the increase of dimensionless seepage resistance by the synergistic effect of well pattern infilling and polymer-surfactant-PPG flooding, and usually shows U-type and gradual-rising W-type response. The rhythm remaining oil and interlayer-controlled remaining oil can be produced by the improvement of water absorption profile and separated layer water injection during polymer-surfactant-PPG flooding, and usually shows gradual-decreasing W-type and early V-type response, respectively.

Declaration of competing interest

The authors declare that they have no known competing financial interests or personal relationships that could have appeared to influence the work reported in this paper.

Acknowledgements

The authors greatly appreciate the financial support of the National Natural Science Foundation of China (Grant No. 52104027), the Project supported by the Joint Funds of the National Natural Science Foundation of China (Grant No. U21B2070), and the Shandong Provincial Natural Science Foundation (Grant No. ZR2021ME072).

References

Bai, B., Li, L., Liu, Y., et al., 2007. Preformed particle gel for conformance control: factors affecting its properties and applications. SPE Reservoir Eval. Eng. 10 (4), 415–422. https://doi.org/10.2118/89389-PA.

Bai, B., Zhou, J., Yin, M., 2015. A comprehensive review of polyacrylamide polymer gels for conformance control. Petrol. Explor. Dev. 42 (4), 525–532. https://doi.org/10.1016/S1876-3804(15)30045-8.

Cao, X., 2013. Design and performance evaluation on the heterogeneous combination flooding system. Acta Pet. Sin. 29 (1), 115–121 (in Chinese).

Cao, X., Guo, L., Wang, H., et al., 2017. The study and pilot on heterogeneous combination flooding system for high recovery percent of reservoirs after polymer flooding. In: The 22nd World Petroleum Congress Held in Istanbul. Turkey. WPC-22-0505.

Du, Q., Pan, G., Hou, J., et al., 2019. Study of the mechanisms of streamline-adjustment-assisted heterogeneous combination flooding for enhanced oil recovery for post-polymer-flooded reservoirs. Petrol. Sci. 16 (3), 606–618. https://doi.org/10.1007/s12182-019-0311-0.

Elsharafi, M.O., Bai, B., 2016. Influence of strong preformed particle gels on low permeable formations in mature reservoirs. Petrol. Sci. 13 (1), 77–90. https://doi.org/10.1007/s12182-015-0072-3.

Farasat, A., Sefti, M.V., Sadeghnejad, S., et al., 2017. Mechanical entrapment analysis of enhanced preformed particle gels (PPGs) in mature reservoirs. J. Petrol. Sci. Eng. 157, 441–450. https://doi.org/10.1016/j.petrol.2017.07.028.

Goudarzi, A., Zhang, H., Varavei, A., et al., 2015. A laboratory and simulation study of preformed particle gels for water conformance control. Fuel 140, 502–513. https://doi.org/10.1016/j.fuel.2014.09.081.

Hou, J., 2007. Network modeling of residual oil displacement after polymer flooding. J. Petrol. Sci. Eng. 59 (3–4), 321–332. https://doi.org/10.1016/j.petrol.2007.04.012.

Hou, J., Du, Q., Shu, Q., et al., 2010. Macroscopic response mechanism and distribution rules of remaining oil in polymer flooding. Acta Pet. Sin. 31 (1), 96–99 (in Chinese).

Hou, J., Du, Q., Lu, T., et al., 2011. The effect of interbeds on distribution of incremental oil displaced by a polymer flood. Petrol. Sci. 8 (2), 200–206. https://doi.org/10.1007/s12182-011-0135-z.

Hou, J., Wu, D., Wei, B., et al., 2019. Percolation characteristics of discontinuous phase and mechanisms of improving oil displacement efficiency in heterogeneous composite flooding. J. China Univ. Petrol. (Ed. Nat. Sci.) 43 (5), 128–135 (in Chinese).

Imqam, A., Bai, B., Delshad, M., 2015. Preformed particle gel propagation through super-k permeability sand and its resistance to water flow during conformance control. In: SPE/IATMI Asia Pacific Oil & Gas Conference and Exhibition. https://doi.org/10.2118/176429-MS.

Imqam, A., Wang, Z., Bai, B., et al., 2016. Effect of heterogeneity on propagation, placement, and conformance control of preformed particle gel treatment in fractures. In: SPE Improved Oil Recovery Conference. https://doi.org/10.2118/179705-MS.

Imqam, A., Wang, Z., Bai, B., 2017. Preformed-particle-gel transport through heterogeneous void-space conduits. SPE J. 22 (5), 1437–1447. https://doi.org/10.2118/179705-PA.

Lu, J., Weerasooriya, U.P., Pope, G.A., 2014. Investigation of gravity-stable surfactant floods. Fuel 124, 76–84. https://doi.org/10.1016/j.fuel.2014.01.082.

Lu, X., Cao, B., Xie, K., et al., 2021. Enhanced oil recovery mechanisms of polymer flooding in a heterogeneous oil reservoir. Petrol. Explor. Dev. 48 (1), 169–178. https://doi.org/10.1016/S1876-3804(21)60013-7.

Ma, Y., Hou, J., Shang, D., et al., 2017. Effect of the loss of viscosity and viscoelasticity on displacement efficiency in polymer flooding. Petrol. Sci. Bull. 2 (1), 133–141 (in Chinese).

Moghadam, A.M., Sefti, M.V., Salehi, M.B., et al., 2012. Preformed particle gel: evaluation and optimization of salinity and pH on equilibrium swelling ratio. J. Pet. Explor. Prod. Technol. 2, 85–91. https://doi.org/10.1007/s13202-012-0024-z.

Qiu, Y., Wei, M., Bai, B., 2017. Descriptive statistical analysis for the PPG field applications in China: screening guidelines, design considerations, and performances. J. Petrol. Sci. Eng. 153, 1–11. https://doi.org/10.1016/j.petrol.2017.03.030.

Saghafi, H.R., Emadi, M.A., Farasat, A., et al., 2016. Performance evaluation of optimized preformed particle gel (PPG) in porous media. Chem. Eng. Res. Des. 112, 175–189. https://doi.org/10.1016/j.cherd.2016.06.004.

Seidy Esfahlan, M., Khodapanah, E., Tabatabaei-Nezhad, S.A., 2021. Comprehensive review on the research and field application of preformed particle gel conformance control technology. J. Petrol. Sci. Eng. 202, 108440. https://doi.org/10.1016/j.petrol.2021.108440.

Sheng, J.J., Leonhardt, B., Azri, N., 2015. Status of polymer-flooding technology. J. Can. Pet. Technol. 54 (2), 116–126. https://doi.org/10.2118/174541-PA.

Song, Z., Bai, B., Zhang, H., 2018. Preformed particle gel propagation and dehydration through semi-transparent fractures and their effect on water flow. J. Petrol. Sci. Eng. 167, 549–558. https://doi.org/10.1016/j.petrol.2018.04.044.

Sun, H., 2014. Application of pilot test for well pattern adjusting heterogeneous combination flooding after polymer flooding: case of Zhongyiqu Ng3 block, Gudao Oilfield. Petrol. Geol. Recovery Eff. 21 (2), 1–4+111. https://doi.org/10.13673/j.cnki.cn37-1359/te.2014.02.001 (in Chinese).

Sun, H., Cao, X., Li, Z., et al., 2020. Research on heterogeneous combination flooding technology based on matching between system and reservoir pore throat and its field application: a case of post-polymer flooding $Es_2$1-3 in Sheng 1 area, Shengtuo Oilfield. Petrol. Geol. Recovery Eff. 27 (5), 53–61. https://doi.org/10.13673/j.cnki.cn37-1359/te.2020.05.006 (in Chinese).

Sun, X., Alhuraishawy, A.K., Bai, B., et al., 2018. Combining preformed particle gel and low salinity water flooding to improve conformance control in fractured reservoirs. Fuel 221, 501–512. https://doi.org/10.1016/j.fuel.2018.02.084.

Wang, R., 2013. Research on Displacement Mechanism and Effect Evaluation for Well Pattern Adjustment with Heterogeneous Combination Flooding after Polymer Flooding. M.Sc. Thesis. China University of Petroleum (East China). (in Chinese).

Wu, D., Zhou, K., Hou, J., et al., 2020. Experimental study on combining heterogeneous phase composite flooding and streamline adjustment to improve oil recovery in heterogeneous reservoirs. J. Petrol. Sci. Eng. 194, 107478. https://doi.org/10.1016/j.petrol.2020.107478.

Zhang, H., Bai, B., 2011. Preformed-particle-gel transport through open fractures and its effect on water flow. SPE J. 16, 388–400. https://doi.org/10.2118/129908-PA.

Zhong, H., He, Y., Yang, E., et al., 2022. Modeling of microflow during viscoelastic polymer flooding in heterogenous reservoirs of Daqing Oilfield. J. Petrol. Sci. Eng. 210, 110091. https://doi.org/10.1016/j.petrol.2021.110091.

Zhou, K., Hou, J., Zhang, X., et al., 2013. Optimal control of polymer flooding based on simultaneous perturbation stochastic approximation method guided by finite difference gradient. Comput. Chem. Eng. 55, 40–49. https://doi.org/10.1016/j.compchemeng.2013.04.009.

Zhou, K., Hou, J., Sun, Q., et al., 2017. An efficient LBM-DEM simulation method for suspensions of deformable preformed particle gels. Chem. Eng. Sci. 167, 288–296. https://doi.org/10.1016/j.ces.2017.04.026.

Zhou, K., Hou, J., Wu, D., et al., 2018. Study on flow diversion caused by deformable preformed particle gel. In: Abu Dhabi International Petroleum Exhibition & Conference. https://doi.org/10.2118/192965-MS.

Zhou, K., Hou, J., Sun, Q., et al., 2019. Study on the flow resistance of the dispersion system of deformable preformed particle gel in porous media using LBM-DEM-IMB method. J. Dispersion Sci. Technol. 40 (10), 1523–1530. https://doi.org/10.1080/01932691.2019.1645028.